

Quantisation Across Bubble Walls and Friction

Aleksandr Azatov^{a,b,c,1}, Giulio Barni^{a,b,2}, Rudin Petrossian-Byrne^{d,3}, Miguel Vanvlasselaer^{e,4}

^a *SISSA International School for Advanced Studies, Via Bonomea 265, 34136, Trieste, Italy*

^b *INFN - Sezione di Trieste, Via Bonomea 265, 34136, Trieste, Italy*

^c *IFPU, Institute for Fundamental Physics of the Universe, Via Beirut 2, 34014 Trieste, Italy*

^d *Abdus Salam International Centre for Theoretical Physics, Strada Costiera 11, 34151, Trieste, Italy*

^e *Theoretische Natuurkunde and IIHE/ELEM, Vrije Universiteit Brussel, & The International Solvay Institutes, Pleinlaan 2, B-1050 Brussels, Belgium*

Abstract

We quantise from first principles field theories living on the background of a bubble wall in the planar limit with particular focus on the case of spontaneous breaking of gauge symmetry. Using these tools, we compute the average momentum transfer from transition radiation: the soft emission of radiation by an energetic particle passing across the wall, with a particular focus on the longitudinal polarisation of vectors. We find these to be comparable to transverse polarisations in symmetry-breaking transitions with mild super-cooling, and dominant in broken to broken transitions with thin wall. Our results have phenomenological applications for the expansion of bubbles during first order phase transitions. Our general framework allows for the robust calculation of any particle processes of interest in such translation breaking backgrounds.

E-mail: ¹aleksandr.azatov@sisssa.it, ²giulio.barni@sisssa.it, ³rpetross@ictp.it, ⁴miguel.vanvlasselaer@vub.be

Contents

1	Introduction	3
2	Simple example: scalars	8
2.1	Complete basis	9
2.2	Quantisation	10
2.3	Out-going eigenstates of momenta	11
2.4	Amplitudes	12
2.5	Phase Space integration	14
2.6	Emission in the WKB regime	15
2.7	Procedure for the momentum transfer calculation: summary	17
2.8	Momentum transfer from scalar emission	19
2.9	Pressure from scalar emission	20
3	Spontaneously broken gauge theories	21
3.1	Particle content in the asymptotic regions	23
3.2	Global degrees of freedom	23
3.2.1	$v \rightarrow 0$ limit	27
3.3	The step wall case	28
3.3.1	(τ) polarisations	29
3.3.2	(λ) polarisation	29
3.4	Quantisation	31
3.5	Subtleties with WKB regime	33
4	Transition radiation and pressure from vectors	35
4.1	Amplitudes	35
4.2	Phase space integration for vector emission	36
4.3	Pressure on the bubble wall	37
5	Summary	42
A	Wavepackets and asymptotic states	44
A.1	Asymptotic states in the wall background	44
A.2	Phase space derivation from wavepackets	46
B	Current conservation in the presence of the wall	47
C	WKB regime in the case of current non-conservation	49
D	Properties of the potential for λ field	49
E	Evaluation of phase space Integrals	51
E.1	Scalars	52
E.2	Vectors: τ emission	53
E.3	$m \neq 0$ asymptotic p^0 regime	53
E.4	The $m \rightarrow 0$ regime	54
E.5	Vectors: λ emission	54

F	Pressure in the EW phase transition	56
G	Sensitivity to wall width	56
H	The suppressed region $\Delta p_z L_w \gg 1$: the Fourier constraint	58

1 Introduction

First-order phase transitions (FOPTs) were proposed long ago as potentially occurring during the hot big-bang phase of the universe [1–3]. In the past, it was entertained that even within the known Standard Model (SM) of particle physics there might have been as many as two: chiral symmetry breaking/confinement in QCD at temperatures $T \sim 150$ MeV and the spontaneous breaking of electroweak (EW) symmetry at $T \sim 160$ GeV. Both are now understood to be smooth crossovers [4, 5]. In fact, it is interesting to note that from the current laws of physics, there is no conclusively established meta-stable vacuum *for any temperature* at zero chemical potential¹.

By contrast, FOPTs are ubiquitous in beyond the SM (BSM) theories. This is due firstly to a vast richness of important phenomenological consequences, among which baryogenesis [7–18], the production of heavy dark matter [19–25], primordial black holes [26–30] and gravitational waves (GW) [3, 31–34] to name a few. In particular, the EW phase transition is easily made first order in many BSM models [14, 35–45] and the consequent out-of-equilibrium dynamics (in conjunction with B violation in the SM) still make for an attractive theory of baryogenesis. Secondly, our currently most compelling picture of physics at the highest energy scales seems to suggest *landscapes* of countless meta-stable vacua. From this perspective, FOPTs may even be expected during the post-inflationary era [46]. Finally, and perhaps most importantly from a phenomenological perspective, the advent of gravitational wave detectors has re-energised interest in these violent phenomena with the prospect of upcoming experiments possibly detecting a stochastic gravitational wave background relic [3, 47, 48]. Thus even FOPTs occurring in potential hidden sectors decoupled from the SM and its thermal history become of interest [49, 50].

A FOPT proceeds through the nucleation and subsequent expansion of bubbles of new phase, pushed by the free-energy density difference ΔV between phases. If friction from the surrounding matter can be ignored, the bubble wall interpolating between the two phases will continue to expand with constant proper acceleration until they collide with each other, with most of the vacuum energy released thus going into kinetic energy of the walls. This scenario is known as *runaway*. If instead friction causes a pressure \mathcal{P} which manages to equilibrate the driving force $\mathcal{P} \simeq \Delta V$, a constant subluminal terminal velocity is reached and energy is efficiently transferred to the medium. All phenomenological consequences listed above, for example, the strength and spectral shape of the stochastic GW signal, depend crucially on the

¹The closest thing that we are aware of is the instability in the Higgs effective potential for central values of SM parameters when extrapolated to very large field range [6]. However, this is sensitive to possible - though unknown - UV physics, over many orders of magnitude, so that we certainly cannot count it as ‘conclusive’.

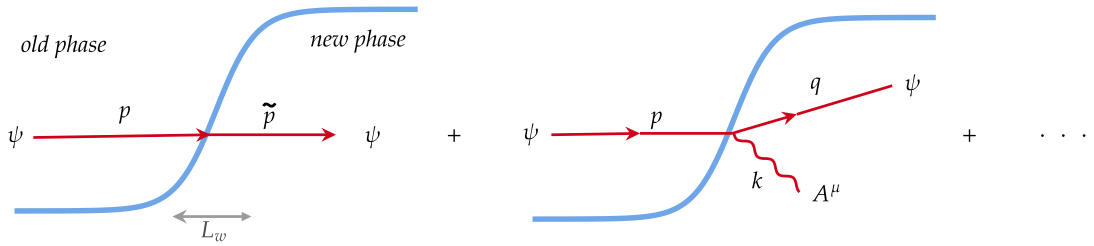


Figure 1: Diagrams corresponding to LO and NLO processes contributing to friction on a moving bubble wall. The emission of vectors with changing mass is generally the dominant $1 \rightarrow 2$ process for friction and the subject of this work. Tilde distinguishes objects in the new phase.

bubble velocity and which of the two regimes is realised. To this end, it becomes important to understand precisely the dynamics of an expanding domain wall in medium². The analysis of bubble-medium interactions is a complicated problem which is largely still under investigation [51–66]. Friction is expected in general to be an involved function of bubble velocity v_w and the surrounding degrees of freedom (d.o.f.). A distinction can be made however between low v_w , when a fluid description is most appropriate, and the ultra-relativistic regime, $\gamma_w \equiv 1/\sqrt{1-v_w^2} \gg L_w \Gamma_{\text{int.}}$, where L_w is the wall thickness in its rest frame and $\Gamma_{\text{int.}}$ is the interaction rate between particles in medium [67]. We will focus on the latter regime in this work, where the wall can be said to be interacting with individual particles.

A particle hitting the wall from the old phase can undergo many processes, which can be organised in terms of a perturbative expansion in couplings of the theory defined in the background of the wall profile, as sketched in fig. 1. The spontaneous breaking of translation symmetry means that momentum perpendicular to the wall is no longer conserved. The average momentum lost $\langle \Delta p \rangle$ times the flux of incoming particles is then the pressure opposing the bubble’s expansion. It is most convenient to work in the rest frame of the wall. At leading order (LO) incoming particles either cross the wall or reflect. It is easy to show that when reflections can be neglected³,

$$\mathcal{P}_{\gamma_w \rightarrow \infty}^{\text{LO}} \simeq (\gamma_w n v_w) \langle \Delta p \rangle \simeq (\gamma_w n v_w) \Delta m^2 / 2 \langle p^0 \rangle, \quad (1)$$

where $\langle p^0 \rangle \propto \gamma_w T$ is the (boosted) incoming particle’s energy in the wall frame, $\Delta m \equiv \sqrt{\tilde{m}^2 - m^2}$ the change in mass between phases, and n the number density in the plasma frame. This LO pressure is independent of γ_w , scaling like $\propto T^2 \tilde{v}^2$ in the case of a thermal bath, where \tilde{v} is the vev in the broken phase⁴ [61, 62].

Later, the same authors analyzed the next-to-LO (NLO) $1 \rightarrow 2$ processes in the same ultra-relativistic regime and found that, despite paying the price of the

²In this work by domain wall we simply mean any bubble wall interpolating between different phases of a theory in the planar limit.

³Although these can be important and even dominant for intermediate relativistic γ_w [68].

⁴This lead to the so-called Bodeker-Moore (BM) criterion $\mathcal{P}^{\text{LO}} < \Delta V$, for the wall to become relativistic. Under the assumption of pressure monotonically increasing with γ_w , the BM criterion was used also as a rough *runaway* condition.

coupling, the emission of soft vector bosons that gain mass during the transition leads to a friction pressure scaling like $\mathcal{P}^{\text{NLO}} \propto \gamma_w$ [63], eventually dominating over the LO effect. This soft emission is known as *transition radiation*. While the original [63] focused on particles emitted forward into the wall (to the right in fig. 1), the authors of [66, 69] considered also reflected emission (to the left in fig. 1) and argued it was larger by a factor of four.

However, all studies after [63] only considered the emission of transverse vector polarisations, ignoring the effects of longitudinal ones. The analysis of these modes is complicated by the rearrangement of particle degrees of freedom across a gauge symmetry breaking transition [70], which has naturally been the case of greatest interest. Moreover, it is well known that amplitudes involving NGBs can give spurious divergences without proper care. Recently it was shown that LO effects from longitudinal modes can have a large impact on pressure [68]. It thus becomes of interest to properly account for their contribution at NLO. In addition, a weakness of the treatments used so far is the frequent reliance on WKB approximations, which are known to break down for the soft momenta dominating the emission phase space.

In this paper, we approach the calculation of transition radiation by quantising field theories in the translation-breaking background of a domain wall from first principles. A complete orthonormal basis is constructed out of ‘left’ and ‘right’ mover energy eigenstates ⁵, each wavemode having ‘reflected’ and ‘transmitted’ parts. We then carefully relate these to *in* and *out* ⁶ asymptotic eigenstates of 4-momentum. In the case of vectors, we show that the degrees of freedom across the wall are most conveniently described in terms of ‘wall polarisations’ τ and λ rather than the conventional transverse and longitudinals, as already pointed out in [70]. The advantage is that $\tau_{1,2}$ and λ are not mixed with each other in the presence of the domain wall. The two sets coincide only for zero transverse momentum $\vec{k}_\perp = 0$ (normal incidence on the wall), where rotations around the direction of propagation are a symmetry ⁷. Moreover, in the case of gauge symmetry breaking, λ smoothly interpolates between a Higgs d.o.f. on the symmetric side and a third massive vector d.o.f. on the broken side. We show how to perform calculations using this basis consistently and avoid divergences which seem to appear in a naive analysis.

Although we explain how to (numerically) compute $\langle \Delta p \rangle$ for a general wall profile, we dedicate most of the work to approximating it in a way that is independent of the particular shape, with the rough scale L_w playing the only role, while commenting on the sensitivity thereon. For the IR of the emitted spectrum $k^z \lesssim L_w^{-1}$ the wall appears effectively as a step function. This limit is particularly interesting theoretically (as well as phenomenologically important, as mentioned already) since everything can be computed analytically and relatively simply. For wavelengths shorter than the wall width $k^z > L_w^{-1}$, the WKB approximation becomes applicable. The integral over the phase space thus splits into two contributions and the averaged

⁵Throughout this paper, the reader should associate ‘right-moving’ with positive z -momentum and ‘left moving’ with negative z -momentum particles.

⁶To be understood in the S matrix language.

⁷Starting from $\vec{k}_\perp = 0$, the general τ and λ polarisation vectors can be obtained by general transverse Lorentz boost - a good symmetry of the theory. Thus orthogonality is obvious. In general, they are also distinguished by whether in unitary gauge the z - component of the vector A^μ is zero or not. See section 3.2.

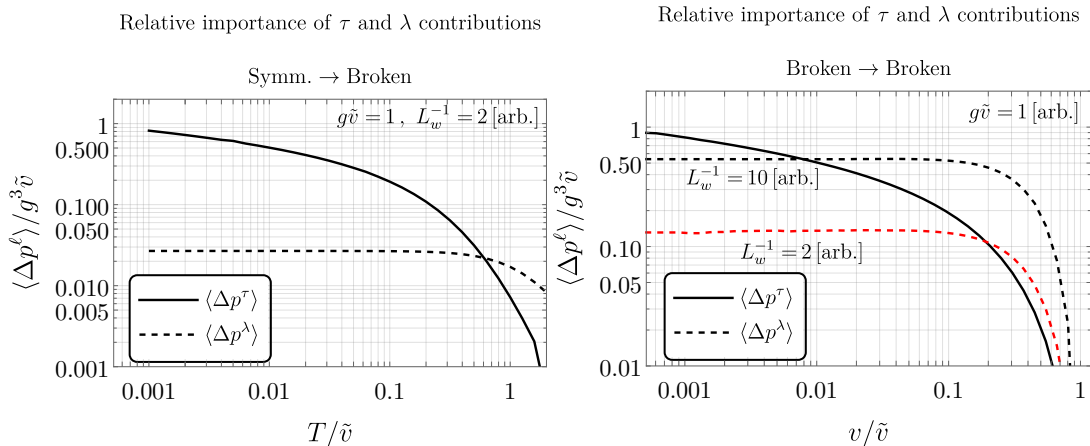


Figure 2: Comparison between the averaged exchanged momentum from transition radiation due to the emission of τ and λ vector polarisations, in the limit of large incoming particle energy $p_0 \rightarrow \infty$. **Left:** Symmetric \rightarrow Broken transition at finite temperature T , shown as a function of temperature over Higgs vev \tilde{v} . T enters via thermal masses (for details see the discussion in section 4.2). Results do not change significantly in the limit $L_w \rightarrow 0$. **Right:** Broken \rightarrow Broken transition. While the τ contribution does not change, λ emission can easily become dominant. We highlight the sensitivity on the wall thickness. [arb.] means arbitrary units.

momentum exchange very schematically takes the form

$$\langle \Delta p \rangle \sim \int^{k^z < L_w^{-1}} d^3 k \Delta p |\mathcal{M}^{\text{step}}|^2 + \int_{k^z > L_w^{-1}} d^3 k \Delta p |\mathcal{M}^{\text{wkb}}|^2. \quad (2)$$

where the \mathcal{M} are matrix elements for emission calculated using the respective approximations. As the incoming flux scales like γ_w , we then have

$$\mathcal{P} \propto \gamma_w \langle \Delta p \rangle. \quad (3)$$

As a warm up, we study transition radiation in a theory with two scalars and observe some surprises. Though we find that the pressure from the emission of one scalar by the other always saturates at large velocities $\mathcal{P}_{\gamma_w \rightarrow \infty}^{\text{NLO, scalars}} \propto \gamma_w^0$, we find also that there can be an intermediate regime of linear growth $\mathcal{P}_{\text{intermediate}}^{\text{NLO, scalars}} \propto \gamma_w$. For scalars we find that the WKB contribution (second term in eq. (2)) dominates the momentum transfer in the asymptotic γ_w limit.

In the case of spontaneous breaking of gauge symmetry we find that the total friction from vector emissions scales as $\propto \gamma_w \log \frac{gT}{\tilde{v}}$ for $T/\tilde{v} \ll 1$, where \tilde{v} is the Higgs' vev, in line with literature. We provide an updated fitted formula in eqs. (136) and (140). The logarithmic enhancement appears only for the τ polarisations, and is dominated by the step function contribution (the first term in the eq. (2)), however we also find that effects of the λ polarisations can lead to significant corrections for mild supercooling ($\frac{\tilde{v}}{T} \sim \text{few}$). We compare the relative importance in fig. 2 (Left). The curves are only very weakly dependent on L_w . This and all of the rest of the figures in the paper are in natural units with some arbitrary scale [arb.].

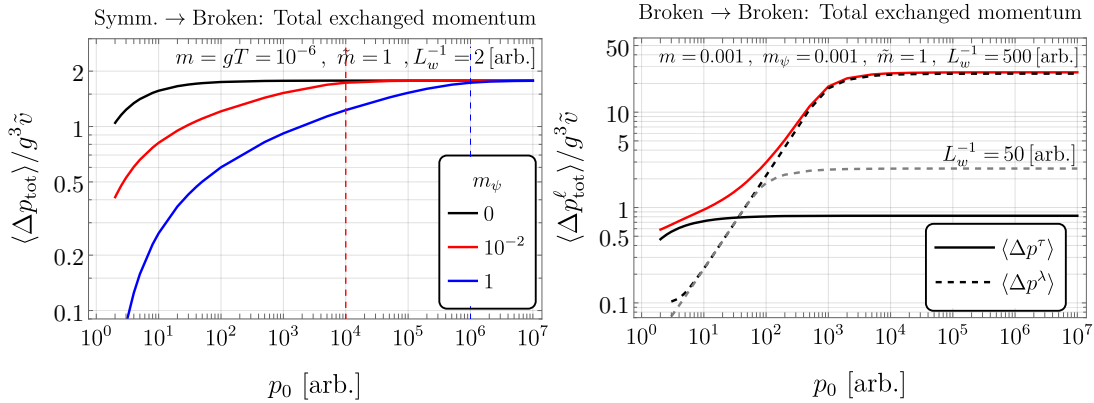


Figure 3: Total averaged momentum exchange as a function of incoming particle energy p^0 . **Left:** Symmetric \rightarrow Broken for different values of the mass of the emitter particle ψ . The asymptotic regime is reached around $p^0 \sim m_\psi \tilde{m}/m$ (dashed lines), with intermediate $\log(p^0/m_\psi)$ growth. **Right:** Broken \rightarrow Broken with thin walls. Here the saturation value is reached around $p_0 \sim L_w^{-1} \text{Max}[1, m_\psi/m]$. Again we highlight the sensitivity to wall width. For small enough L_w we find an inter-relativistic regime with averaged exchange momentum growing linearly, which translates to pressure scaling like γ_w^2 .

As a side application, we also compute the transition radiation when the bubble wall connects two vacua with broken gauge symmetry but different vevs v and \tilde{v} . In this case, the contribution to friction from the longitudinal vector emission scales as $\mathcal{P}_{\gamma_w \rightarrow \infty}^{\text{NLO, vectors}} \propto \gamma_w L_w^{-1}$ (see fig. 2, Right) and can dominate over the transverse for thin wall.

Aside from the asymptotic $p^0 \rightarrow \infty$ limit, we are also able to explore regimes with intermediate - though large - γ_w . For symmetric \rightarrow broken transition we find that the saturating value is reached at energies dependent on the mass of the emitter particle, as shown in fig. 3 (Left). In the case of the broken \rightarrow broken transition we find that there is an intermediate regime where the pressure scales as $\mathcal{P}_{\text{intermediate}}^{\text{NLO, vectors}} \propto \gamma_w^2$ (right panel of fig. 3).

The paper is organised as follows: in the section 2 we work through a toy model with only scalars, introducing various elements of the calculation. In section 3 we quantise an Abelian Higgs model in the presence of a symmetry breaking domain wall and present the results for transition radiation of vectors in section 4. We summarise in section 5.

Summary of notation: In the rest of this paper, we will adopt the following conventions:

1. We treat the bubble wall in the planar limit, where it is one dimensional and centred around $z = 0$.
2. We use a hybrid notation for four-vector Lorentz indices:
 $\mu = (n, z) \equiv (0, 1, 2, z)$. Coordinates are $x^\mu = (x^n, z) \equiv (t, \vec{x}_\perp, z)$.

3. Similarly for momenta $k^\mu = (k^n, k^z) \equiv (k_0, \vec{k}_\perp, k^z) \equiv (k_0, \vec{k})$.
Also $E^2 = k^n k_n = k_0^2 - k_\perp^2$, where $k_\perp = |\vec{k}_\perp|$.
4. We define the change in mass across the wall $\Delta m \equiv \sqrt{\tilde{m}^2 - m^2}$.
5. L_w is the thickness of the wall.
6. $\gamma_w (v_w)$ is the boost factor (the velocity) of the wall.
7. The momenta p, q, k will always be used as in fig. 1 and we define:

$$\begin{aligned}\Delta p &\equiv p^z - q^z - k^z, & \Delta p_r &\equiv p^z - q^z + k^z, \\ \Delta \tilde{p} &\equiv p^z - q^z - \tilde{k}^z, & \Delta \tilde{p}_r &\equiv p^z - q^z + \tilde{k}^z.\end{aligned}\tag{4}$$

2 Simple example: scalars

In this section, as a warm up for the more complex case of gauge theories, we go through the quantisation of a scalar field theory in the presence of a domain wall and derive results for transition radiation for the case of one scalar emitting another. This toy example is sufficient to highlight many features of calculations in a spatially dependent background.

Consider two different scalar fields ϕ, ψ , the first of which feels the wall and has different mass depending on the phase, while the second for simplicity does not. The Lagrangian we consider is the following

$$\mathcal{L} = \frac{1}{2}(\partial\phi)^2 + \frac{1}{2}(\partial\psi)^2 - \frac{1}{2}m_\phi^2(z)\phi^2 - \frac{1}{2}m_\psi^2\psi^2 - y(z)\frac{1}{2}\psi^2\phi,\tag{5}$$

where $m(z)$ interpolates between $m^2(z)|_{z\rightarrow-\infty} = m^2 = \text{const}$ and $m^2(z)|_{z\rightarrow+\infty} = \tilde{m}^2 = \text{const}$. Similarly $y(z)$ goes from y to \tilde{y} . The profiles change on the scale of the wall width L_w around $z = 0$. The interactions in eq. (5) are not the most general, but are designed to mimic the vector case when $y = \text{const}$. The process that we will be studying is $\psi \rightarrow \psi\phi$, which would be forbidden by kinematics if it was not for the breaking of z -momentum.

Section summary: In section 2.1 and 2.2, we quantise the free theory, focusing on the ϕ field ⁸, by defining a complete basis of solutions that solve its equations of motion. In section 2.3, we define a new basis that corresponds to *out-going* eigenstates of momentum. Later, in section 2.4, we calculate the amplitude for the $\psi \rightarrow \psi\phi$ transition in the step wall approximation, valid when $k^z L_w \lesssim 1$. In section 2.5, we present the proper domain for the phase space integration over the final state. In section 2.6, we complete the emission spectrum discussing the calculation of the amplitude in the (opposite) WKB regime $k^z L_w \gtrsim 1$. In section 2.7, we summarise and present master formulae for the calculation of the averaged momentum transfer $\langle \Delta p \rangle$. We conclude by discussing results for $\langle \Delta p \rangle$ and pressure \mathcal{P}^{NLO} in sections 2.8 and 2.9 respectively.

⁸The quantisation of ψ , as it does not feel the wall, is instead completely standard.

2.1 Complete basis

The quantisation of modes in the presence of a background profile arises in many corners of physics. A very similar task appears for example in the quantisation of field theory in black hole spacetimes. We found the treatment in [71] particularly useful. In the simple example of eq. (5) above, the discussion is relevant for ϕ , which satisfies

$$(\partial^2 + m_\phi^2(z))\phi = 0, \quad (6)$$

with a z -dependent mass term. To perform second quantisation we need to first find a convenient basis of solutions of this equation. Far away from the wall the solutions are plane waves. A convenient choice of complete orthonormal basis is given in terms of ‘right’ and ‘left’ moving solutions, which are defined by their boundary conditions as follows⁹

$$\phi_{R,k} = e^{-ik_n x^n} \chi_{R,k}(z) \equiv e^{-ik_n x^n} \begin{cases} e^{ik^z z} + r_{R,k} e^{-ik^z z}, & z \rightarrow -\infty \\ t_{R,k} e^{i\tilde{k}^z z}, & z \rightarrow +\infty \end{cases} \quad (\text{Right}) \quad (7)$$

with $k^0 > m$ and

$$\phi_{L,k} = e^{-ik_n x^n} \chi_{L,k}(z) \equiv e^{-ik_n x^n} \sqrt{\frac{k^z}{\tilde{k}^z}} \begin{cases} t_{L,k} e^{-ik^z z}, & z \rightarrow -\infty \\ r_{L,k} e^{i\tilde{k}^z z} + e^{-i\tilde{k}^z z}, & z \rightarrow +\infty \end{cases} \quad (\text{Left}) \quad (8)$$

with $k^0 > \tilde{m}$ and we take k^z, \tilde{k}^z to be strictly positive¹⁰. The factor $\sqrt{k^z/\tilde{k}^z}$ is included in eq. (8) to ensure appropriate normalisation (see below, eq. (14)). In the limit of no domain wall the r_L, r_R (t_L, t_R) coefficients are zero (one) and ϕ_L, ϕ_R correspond simply to the plane waves with $\mp k^z$ momenta. The momentum along z is not conserved across the wall; however, asymptotically far it becomes constant and fixed by the relations

$$k^z \equiv \sqrt{k_0^2 - k_\perp^2 - m^2}, \quad \tilde{k}^z \equiv \sqrt{k_0^2 - k_\perp^2 - \tilde{m}^2}. \quad (9)$$

In general, we need to solve the equations of motion to find the expression of the coefficients $r_{L,R}, t_{L,R}$. Consequently, they will depend on the explicit form of the mass variation $m_\phi^2(z)$. However, here it will be sufficient to consider the *step wall* ansatz for the mass $m_\phi^2(z)$

$$m_\phi^2(z) = m^2 + \Delta m^2 \Theta(z), \quad \Delta m^2 \equiv \tilde{m}^2 - m^2. \quad (10)$$

using the Heaviside Theta function. The form of the coefficients for the scalar case under consideration can be obtained by matching ϕ and its first derivative at the origin $z = 0$, where the step wall lies. They take the form

$$r_{R,k} = \frac{k^z - \tilde{k}^z}{k^z + \tilde{k}^z}, \quad t_{R,k} = \frac{2k^z}{k^z + \tilde{k}^z}. \quad (11)$$

⁹Recall that the index n designates 0, 1, 2 and not the z direction.

¹⁰As is well known, the basis formed by just $\phi_{R,k}$ but allowing k^z to take both signs (and $\tilde{k}^z = \text{sign}(k)(\sqrt{k^2 - \Delta m^2})$) is also complete but not orthogonal and therefore less convenient. For example, the algebra of creation and annihilation operators would be more complicated.

These expressions are specific to the step-wall assumption. However, the general treatment that we present here will hold for general r_k, t_k coefficients and could be easily adapted to a smooth wall case. Modes with $m < k_0 < \tilde{m}$ decay exponentially on the right of the wall and are automatically included as right-movers. For these, \tilde{k} is purely imaginary with magnitude

$$|\tilde{k}^z|^2 = \Delta m^2 - k_z^2 \quad \text{for} \quad 0 < k^z < \Delta m . \quad (12)$$

In a similar fashion, for the left moving solution we find

$$r_{L,k} = -r_{R,k} = \frac{\tilde{k}^z - k^z}{k^z + \tilde{k}^z} , \quad t_{L,k} = \frac{\tilde{k}^z}{k^z} t_{R,k} = \frac{2\tilde{k}^z}{k^z + \tilde{k}^z} . \quad (13)$$

and we explicitly note the condition $k_0 > \tilde{m}$, to avoid the inclusion of solutions growing exponentially at infinity. The left and right moving modes are orthonormal in the sense that

$$\int_{-\infty}^{\infty} dz \chi_{I,k} \chi_{J,q}^* = 2\pi \delta_{IJ} \delta(k^z - q^z) , \quad I, J \in \{R, L\} . \quad (14)$$

Computing integrals such as eq. (14) in the step function case requires the identity

$$\int_{-\infty}^0 e^{i\beta z} dz = \text{PV} \left(\frac{1}{i\beta} \right) + \pi \delta(\beta) , \quad (15)$$

and its complex conjugate (which gives the integral from 0 to ∞). In eq. (14) the principle value (PV) pieces vanish as soon as we specify the relation between \tilde{k}^z and k^z , i.e. $\tilde{k}_z^2 = k_z^2 + m^2 - \tilde{m}^2$. Notice we can discard terms proportional to $\delta(k^z + q^z)$ due to the strictly positive definition of k^z, q^z in our definition. If explicitly computing things like the Hamiltonian and operator algebra (see next subsection) it is also useful to know the other inner products:

$$\begin{aligned} \int_{-\infty}^{\infty} dz \chi_{R,k} \chi_{R,q} &= - \int_{-\infty}^{\infty} dz \chi_{L,k} \chi_{L,q} = 2\pi \frac{k^z - \tilde{k}^z}{k^z + \tilde{k}^z} \delta(k^z - q^z), \\ \int_{-\infty}^{\infty} dz \chi_{R,k} \chi_{L,q} &= 4\pi \frac{\sqrt{k^z \tilde{k}^z}}{k^z + \tilde{k}^z} \delta(k^z - q^z). \end{aligned} \quad (16)$$

Finally, we would like to comment that, in general, bound states may also appear in the spectrum, in addition to the scattering states studied above, if the function $m_\phi^2(z)$ is non-monotonic and has minima in the vicinity of the domain wall. These are of the form $\phi_b \propto e^{-ik^n x_n} \chi_b(z)$, with χ_b exponentially decaying for $|z| \rightarrow \infty$ and should be included in the upcoming expansion eq. (17).

2.2 Quantisation

Now that we have a complete orthonormal basis of eigenstates in the presence of the wall, we can proceed to quantise the theory. The field ϕ can be expanded in the

form ¹¹

$$\phi(x, t) = \sum_{I=R,L} \int \frac{d^3k}{(2\pi)^3 \sqrt{2k_0}} \left(a_{I,k} \phi_{I,k} + a_{I,k}^\dagger \phi_{I,k}^* \right),$$

where $\phi_{L,k} \equiv 0$ for $E < \tilde{m}$, (17)

where $d^3k \equiv dk^z d^2k_\perp$, we recall $E \equiv \sqrt{k_0^2 - k_\perp^2}$ and k^z runs between $[0, \infty)$. We choose to label states by their quantum numbers outside the wall¹². Note we have trivially extended the definition of the left moving modes to the region $E < \tilde{m}$ for convenience.

Using eqs. (14) and (16), one can show that

$$a_{I,p} = \int \frac{dz}{\sqrt{2p_0}} e^{ip_0 t} \chi_{I,p}^* (i\pi + p_0 \phi),$$
(18)

where $\pi \equiv \partial_t \phi$. Promoting Poisson brackets of ϕ and its conjugate momentum π to canonical commutation relations gives the familiar commutation algebra

$$\begin{aligned} [a_{I,k}, a_{J,q}^\dagger] &= (2\pi)^3 \delta(\vec{k} - \vec{q}) \delta_{IJ}, \\ [a_{I,k}, a_{J,q}] &= [a_{I,k}^\dagger, a_{J,q}^\dagger] = 0, \quad I, J \in \{R, L\}. \end{aligned}$$
(19)

We can define two types of states

$$|k_R\rangle \equiv \sqrt{2k_0} a_{R,k}^\dagger |0\rangle,$$
(20)

$$|k_L\rangle \equiv \sqrt{2k_0} a_{L,k}^\dagger |0\rangle,$$
(21)

which should be thought of as independent external states in any process. The space of physical states is thus the *Fock* space defined by arbitrary powers of $a_{R,k}^\dagger$ and $a_{L,k}^\dagger$ acting on the vacuum.

2.3 Out-going eigenstates of momenta

In the previous subsections we chose to quantise the orthonormal basis $\{\phi_{R,k}, \phi_{L,k}\}$ and defined associated one-particle states $|k_R\rangle$ and $|k_L\rangle$. As we explain in more detail in appendix A by the use of wave-packets, these should be thought of as describing incoming particles with definite z -momenta k^z and $-\tilde{k}^z$ respectively at $t \rightarrow -\infty$, but at $t \rightarrow +\infty$ they correspond to a superposition between a transmitted and reflected particle. As a consequence, the functions $\phi_{R,L}$ are eigenstates of momenta only at $t \rightarrow -\infty$. They are well-suited for processes with asymptotic *in-state* ϕ particles.

On the other hand, in this work we will be interested in the momentum transfer to the wall, so it is more convenient to have a ϕ particle emitted as an asymptotic

¹¹We use normalisation conventions in line with [72].

¹²This is more convenient than labeling with respect to \tilde{k}^z since this becomes imaginary for the branch $0 < k^z < \Delta m$.

out-state with well-defined momentum at $t \rightarrow \infty$. A complete orthonormal basis of such late-time eigenstates of momentum is given by

$$\phi_{L,k}^{\text{out}} \equiv e^{-ik_n x^n} \zeta_{L,k}(z) = e^{-ik_n x^n} \chi_{R,k}^*(z) = e^{-ik_n x^n} \left(r_{R,k}^* \chi_{R,k} + t_{R,k}^* \sqrt{\frac{\tilde{k}^z}{k^z}} \chi_{L,k} \right), \quad (22)$$

$$\phi_{R,k}^{\text{out}} \equiv e^{-ik_n x^n} \zeta_{R,k}(z) = e^{-ik_n x^n} \chi_{L,k}^*(z) = e^{-ik_n x^n} \left(r_{L,k}^* \chi_{L,k} + t_{L,k}^* \sqrt{\frac{k^z}{\tilde{k}^z}} \chi_{R,k} \right), \quad (23)$$

where in the last equalities we related them to the basis of section 2.1. We emphasise again that in our notation $k^z, \tilde{k}^z > 0$ always. $\phi_{L,k}^{\text{out}}$ and $\phi_{R,k}^{\text{out}}$ should be thought of as describing an outgoing final state particle with $-k^z$ and $+\tilde{k}^z$ momentum respectively. Recall that the function $\chi_{L,k}$ vanishes for $k^z < \Delta m$ and the corresponding Θ functions are implicit. At $t \rightarrow -\infty$ they are both superpositions of incoming particles from $z = \pm\infty$ and do not have well defined momentum. In practice we need to calculate the amplitudes with $\zeta_{L,R} = \chi_{R,L}^*$ wave functions. At the level of states, we have

$$|k_L^{\text{out}}\rangle = r_{R,k}^* |k_R\rangle + t_{R,k}^* \sqrt{\tilde{k}^z/k^z} |k_L\rangle \Theta(k^z - \Delta m), \quad (24)$$

$$|k_R^{\text{out}}\rangle = t_{L,k}^* \sqrt{k^z/\tilde{k}^z} |k_R\rangle + r_{L,k}^* |k_L\rangle, \quad (25)$$

where we explicitly remind ourselves that when $0 < k^z < \Delta m$ the left mover state does not exist. The different asymptotic states are illustrated in the fig. 4.

We emphasise that both bases can be used to quantise the theory. In our present paper however we will consider only outgoing ϕ particles so that the basis $\{\phi_{R,k}^{\text{out}}, \phi_{L,k}^{\text{out}}\}$ is actually more convenient. From now on we drop the label ‘out’ and we will refer to R (L) emission meaning using the mode functions $\{\zeta_R, \zeta_L\}$, if not stated otherwise.

2.4 Amplitudes

We now finally turn to compute the amplitude for the process $\psi \rightarrow \psi\phi$ in the background of a domain wall. We have not discussed the quantisation of ψ since it does not feel the wall directly and there are no complications with respect to the standard theory. In the previous sections we argued that there are two processes we have to consider separately: the emission of a left and right moving ϕ particle, with respective wavefunctions $\zeta_L(\zeta_R)$. Having quantised the free theory, the treatment of perturbative interactions proceeds as standard, by defining an S -matrix in terms of the interaction Hamiltonian $\mathcal{S} = \text{T exp}(-i \int d^4x \mathcal{H}_{\text{Int}})$ where T here denotes time ordering. We have the amplitudes of interest

$$\langle k_I^{\text{out}} q | \mathcal{S} | p \rangle \equiv (2\pi)^3 \delta^{(3)}(p^n - k^n - q^n) i \mathcal{M}_I \stackrel{\text{tree}}{=} -i \int d^4x \langle k_I^{\text{out}} q | \mathcal{H}_{\text{Int}} | p \rangle \quad (26)$$

with $I = L, R$,

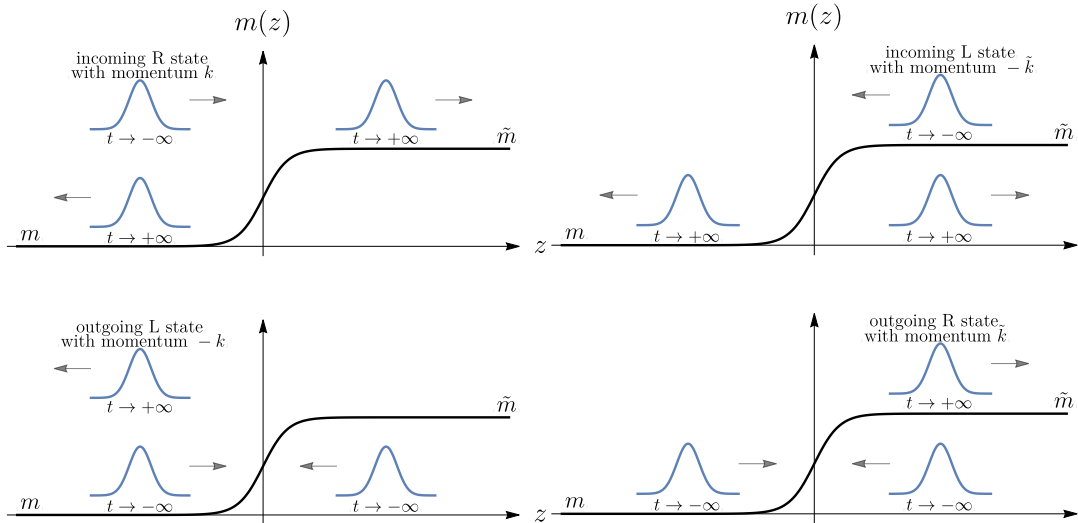


Figure 4: Summary of asymptotic external states with definite 4-momentum, to be used in calculating any process in the background of a domain wall (or any localised z -dependent potential). The upper panels represent in-state particles incoming from $z = -\infty$ and $z = \infty$. In the plane wave limit they correspond to states $|k_R\rangle$ and $|k_L\rangle$ with wavefunctions eqs. (7) and (8) respectively. The lower panels represent out-state particles travelling out towards $z = -\infty$ and $z = \infty$. They correspond to states eqs. (24) and (25) with wavefunctions eqs. (22) and (23) respectively.

where p and q stand for the initial and final one particle states for the ψ field and their respective 4-momenta, and the last equality is up to leading order in perturbation theory (tree level). Notice we have defined the matrix element \mathcal{M} as closely as possible to standard theory. Of course, we cannot extract a z -momentum conserving delta function but rather \mathcal{M} still contains the integral over z .

For the theory of scalars of eq. (5), we have $\mathcal{H}_{\text{Int}} = -iy\psi^2(x)\phi(x)$ and we can now proceed to explicitly computing amplitudes. In the case of a ζ_L mode emission (where the emitted scalar has $-k^z$ momentum), the amplitude takes the form

$$\begin{aligned} \mathcal{M}_L &= \int_{-\infty}^{\infty} dz y(z) e^{i(p^z - q^z)z} [\zeta_{L,k} = \chi_{R,k}^*(z)]^* \\ &= \left[\frac{-iy}{p^z - q^z + k^z} + r_{R,k} \frac{-iy}{p^z - q^z - k^z} - t_{R,k} \frac{-i\tilde{y}}{p^z - q^z + \tilde{k}^z} \right]. \end{aligned} \quad (27)$$

Instead, in the case of ζ_R mode emission (where the emitted scalar has $+\tilde{k}^z$ momentum):

$$\begin{aligned} \mathcal{M}_R &= \int_{-\infty}^{\infty} dz y(z) e^{i(p^z - q^z)z} [\zeta_{R,k} = \chi_{L,k}^*(z)]^* \\ &= \sqrt{\frac{k^z}{\tilde{k}^z}} \left[t_{L,k} \frac{-iy}{p^z - q^z - k^z} - \frac{-i\tilde{y}}{p^z - q^z - \tilde{k}^z} - r_{L,k} \frac{-i\tilde{y}}{p^z - q^z + \tilde{k}^z} \right], \end{aligned} \quad (28)$$

where the square root factor comes from the normalisation condition in eq. (8). To compute the total friction from $\psi \rightarrow \psi\phi$ we must sum the contributions from

both processes. Then we can compute the amplitude squared for the emission of a right/left mover, under the assumption that $y = \text{const.}$, we obtain

$$|\mathcal{M}_R|^2 = y^2 \frac{4k^z \tilde{k}^z (k^z - \tilde{k}^z)^2}{(\tilde{k}_z^2 - (p^z - q^z)^2)^2 (k^z - p^z + q^z)^2}, \quad (29)$$

$$|\mathcal{M}_L|^2 = y^2 \frac{4k_z^2}{(k_z^2 - (p^z - q^z)^2)^2} \begin{cases} \frac{(k^z - \tilde{k}^z)^2}{(k^z + p^z - q^z)^2}, & k^z > \Delta m, \\ \frac{\Delta m^2}{\Delta m^2 - k_z^2 + (p^z - q^z)^2}, & k^z < \Delta m, \end{cases} \quad (30)$$

where for L emission we distinguished between the two branches corresponding to \tilde{k}^z purely real and imaginary, and used eq. (12) to simplify in the latter case.

2.5 Phase Space integration

We can now compute the average exchanged momentum due to transition radiation, $\langle \Delta p \rangle$ due to a single incoming particle. We integrate over the whole allowed phase space of the final two particles, weighting the amplitude squared for ψ to emit ϕ by the momentum lost. We add separately contributions from left and right movers with their respective slightly different phase space. $\langle \Delta p \rangle(p)$ is in general a function of the four-momentum p of the incoming ψ . From $\langle \Delta p \rangle$ we can compute the total friction pressure by integrating over the incoming flux.

For simplicity we take $\vec{p}_\perp = 0$ and parameterise the kinematics of the $1 \rightarrow 2$ process as follows

$$\begin{aligned} p^\mu &= (p_0, 0, 0, \sqrt{p_0^2 - m_\psi^2}), & q^\mu &= (q_0, -k_\perp, 0, q^z), \\ k^\mu &= (k_0, k_\perp, 0, k^z), & \tilde{k}^\mu &= (k_0, k_\perp, 0, \tilde{k}^z), \end{aligned} \quad (31)$$

where \tilde{k}^z is defined in eq. (9) and $q^z = \sqrt{q_0^2 - k_\perp^2 - m_\psi^2}$, with $q_0 = p_0 - k_0$ from energy conservation. Note we have used the cylindrical symmetry of the set up to make the second spatial component of k^μ zero. $\langle \Delta p \rangle$ is given by the sum of left and right contributions

$$\begin{aligned} \langle \Delta p \rangle &= \langle \Delta p_R \rangle + \langle \Delta p_L \rangle \\ &\equiv \int d\mathbb{P}_{\psi \rightarrow \psi \phi_R} \underbrace{(p^z - q^z - \tilde{k}^z)}_{\Delta p_R^z} + \int d\mathbb{P}_{\psi \rightarrow \psi \phi_L} \underbrace{(p^z - q^z + k^z)}_{\Delta p_L^z}. \end{aligned} \quad (32)$$

where $d\mathbb{P}_{\psi \rightarrow \psi \phi_I}$ is the differential probability. The first and second terms on the RHS of eq. (32), will be different in their lower limits on the k^z integrals. The second term, left-mover emission, contains also the modes $k^0 < \tilde{m}$ which are exponentially decaying inside the wall. In appendix A.2 we show that

$$\int d\mathbb{P}_{\psi \rightarrow \psi \phi_I} \Delta p_I^z = \int_{k_{\min}^{z,I}}^{k_{\max}^{z,I}} \frac{dk_z}{2\pi} \frac{1}{2k_0} \int_0^{k_{\perp, \max}^2} \frac{dk_\perp^2}{4\pi} \cdot \frac{1}{2p^z} \left[\frac{1}{2|q^z|} |\mathcal{M}_I|^2 \Delta p_I^z \right]_{q^z = \pm q_k^z}, \quad (33)$$

where $I = R, L$ and $[\dots]_{q^z = \pm q_k^z}$ is intended to be the sum over $q^z = \pm q_k^z$. The contribution with $q^z = -q_k^z$ corresponds to the reflection of the incoming particle ψ ,

a branch missing in the previous literature. Of course, in the ultra-relativistic regime, it is expected that this should be highly suppressed¹³. The limits of integration of eq. (33) are found demanding the reality of the q^z momentum, obtaining for the (R) modes

$$\begin{aligned} \text{(Right)} : k_{\min}^{z,R} &\equiv \Delta m \leq k^z \leq k_{\max}^z \equiv \sqrt{(p_0 - m_\psi)^2 - m^2}, \\ 0 \leq k_\perp^2 &\leq k_{\perp,\max}^2 \equiv \frac{1}{4p_0^2} (p_0^2 + k_z^2 + m^2 - m_\psi^2)^2 - k_z^2 - m^2. \end{aligned} \quad (34)$$

For the (L) modes, the only difference is

$$\text{(Left)} : k_{\min}^{z,L} \equiv 0 \leq k^z \leq k_{\max}^z. \quad (35)$$

Following this discussion, in general, there will be four contributions:

$$\langle \Delta p_L^{q^z < 0} \rangle, \langle \Delta p_L^{q^z > 0} \rangle, \langle \Delta p_R^{q^z < 0} \rangle, \langle \Delta p_R^{q^z > 0} \rangle.$$

However, we explicitly checked that in all cases of interest, the contributions with $q^z < 0$ are largely subdominant and we will ignore them completely in the rest of this paper.

2.6 Emission in the WKB regime

So far we have been treating the bubble wall as a step function. This is a good approximation if the z momentum of the emitted particle is less than the inverse scale over which the background (in the case of eq. (5), the mass) changes significantly, i.e. $k^z \lesssim L_w^{-1}$. How can we proceed if the particles' momentum becomes comparable or larger than the width of the wall? First of all, if we know the shape of the potential exactly, we can solve for the left and right mover solutions as we did above for the step-wall, and proceed with these functions in precisely the same way as before. In principle, this can always be done numerically. However, we will argue that even in the case when we do not know the exact shape of the potential, we can still obtain reliable results.

Let us consider a particle hitting the wall with momentum $k^z \gg L_w^{-1}$. Reflection will be suppressed and the WKB approximation, which has been used extensively in the literature [63, 65, 66], becomes applicable. The approximate form of the z -dependent wavefunctions are now $\chi \approx \sqrt{k^z(z_0)/k^z(z)} e^{\pm i \int_{z_0}^z k^z(z') dz'}$, with z_0 some reference position. Having the approximate solutions to the $\chi_{R,L}(\zeta_{R,L})$ basis functions, we proceed in the same way as in section 2.4. Thus, in practice this means separating the phase space into two regions:

$$\begin{aligned} \text{region (1)} & \quad k_\phi^z \ll L_w^{-1}, \quad \text{step wall,} \\ \text{region (2)} & \quad k_\phi^z \gg L_w^{-1} \quad \text{WKB.} \end{aligned} \quad (36)$$

¹³Notice that the sign change in Δp_R^z means that a process with $q^z < 0$ contributes more to momentum exchange, but it is the amplitude which is generally suppressed.

In the WKB regime the amplitude for a general $1 \rightarrow$ many right-movers¹⁴ process, allowing for all masses to vary, can be schematically written as follows

$$\mathcal{M}_{\text{wkb}} = \int_{-\infty}^{+\infty} dz V(z) \exp \left[i \int_0^z \Delta p(z') dz' \right] \prod_i \sqrt{\frac{p_z^i(0)}{p_z^i(z)}},$$

$$\Delta p(z') \equiv p^z(z') - \sum_i p_i^z(z') = p^z(z') - \sum_i \sqrt{(p_0^i)^2 - (p_\perp^i)^2 - m_i^2(z')}, \quad (37)$$

where i sums over final state particle momenta. Naively, computing this integral requires knowledge of the functions $m_i(z)$. However, these are changing only in the vicinity of the wall, while outside they quickly reach the asymptotic constant values. This means we can split the amplitude into two pieces

$$\mathcal{M}^{\text{wkb}} = \underbrace{\int_{-\infty}^0 dz V(-\infty) e^{i\Delta p_z(-\infty)z} + e^{i \int_0^{L_w} dz' \Delta p(z')} \int_0^\infty dz V(+\infty) e^{i\Delta p_z(+\infty)z}}_{\mathcal{M}_{\text{outside}}} + \underbrace{\int_0^{L_w} dz V(z) e^{i \int_0^z dz' \Delta p(z')}}_{\mathcal{M}_{\text{inside}}}, \quad (38)$$

where the assumption is that things are varying only between $z \in [0, L_w]$. In the WKB regime, all the momenta of the particles are much larger than the inverse width of the wall $p^z L_w \gg 1$ so the overall modification of momenta $p(+\infty) - p(-\infty) \ll p(\infty)$ is much less than its absolute value (if the wall is not too thick $m(z)L \lesssim 1$), this is why we have approximated $\prod \sqrt{p/p(z)} \rightarrow 1$. Similarly $\Delta p(+\infty) - \Delta p(-\infty) \ll \Delta p(\infty)$, then from basic properties of Fourier transformations the amplitude

$$\mathcal{M} \rightarrow 0, \text{ if } \Delta p_z^{\text{max}} L_w \gg 1, \quad (39)$$

with $\Delta p_z^{\text{max}} = \text{Max}[\Delta p_z(\pm\infty)]$. The physics behind this relation is very simple: the wall of the width L_w can lead to the momentum loss Δp_z at most L_w^{-1} . This is expected since the processes with $\Delta p_z \gg L_w^{-1}$ happen at distances $\sim \Delta p_z^{-1}$, much shorter than the typical wall width. However, at such small distances we recover translational symmetry along the z direction and transition radiation must be forbidden (we checked these statements for various wall ansatzes in appendix H). From these arguments, we can see that independently of the wall ansatz the particle emission will be dominated by the region $\Delta p_z L_w \lesssim 1$. Then we can approximate the amplitude as follows

$$\mathcal{M}^{\text{wkb}} = \int_{-\infty}^0 dz V(-\infty) e^{i\Delta p_z(-\infty)z} + \int_0^\infty dz V(+\infty) e^{i\Delta p_z(+\infty)z} + \int_0^{L_w} dz V(z) e^{i \int dz \Delta p(\tilde{z})}. \quad (40)$$

¹⁴We will see later on how left mover emission is negligible for us in the WKB regime.

Performing the z integrals for the first two terms is trivial and, using eq. (15), we get

$$\mathcal{M}^{\text{wkb}} \approx \frac{V(-\infty)}{i\Delta p_z(-\infty)} - \frac{V(+\infty)}{i\Delta p_z(+\infty)} + \int_0^{L_w} dz V(z) e^{i \int dz \Delta p(z)} \quad (41)$$

The last term scales very roughly as $V(z \in [0, L_w])L_w$ then assuming $V(z \in [0, L_w]) \sim V(\infty) \sim V(-\infty)$ we can see it will be suppressed by the condition $\Delta p L_w \lesssim 1$. Thus we arrive at the Bodeker-Moore formula [63] for reduced matrix element

$$\mathcal{M}^{\text{wkb red.}} = \frac{V(-\infty)}{i\Delta p_z(-\infty)} - \frac{V(+\infty)}{i\Delta p_z(+\infty)}. \quad (42)$$

Now one can take this formula and perform the phase space integration. However, we would like to emphasise a simple but important point. Since we have ignored the contribution inside the wall, there is no guarantee that the matrix element will be suppressed in the region with $\Delta p_z L_w \gg 1$. In all of our calculations we always:

- impose $\Delta p_z L_w < 1$ – Fourier decomposition properties
- verify that $\mathcal{M}_{\text{inside}} \ll \mathcal{M}_{\text{outside}}$ – applicability of BM approximation (we will see that satisfying this inequality turns out to be non-trivial for longitudinal vector bosons).

Finally, from this discussion it is clear that we should not worry about left emission in the WKB regime since for left movers with $k^z > L_w^{-1}$ the total loss of momenta $\Delta p_z = p^z - q^z + k^z > L_w^{-1}$, meaning these processes must be strongly suppressed and we can safely ignore them.

Scalars example Let us apply this very generic discussion to the case of scalar radiation. Then the matrix element will be given by

$$\mathcal{M}^{\text{wkb red.}} = \frac{-iy}{p^z - q^z - k^z} - \frac{-iy}{p^z - q^z - \tilde{k}^z}, \quad (43)$$

for the contribution outside of the wall. The contribution inside the wall (which we ignore) scales roughly as

$$\frac{\mathcal{M}_{\text{wkb}}^{\text{inside}}}{\mathcal{M}^{\text{wkb red.}}} \sim \Delta p_z L_w, \quad (44)$$

which is always less than one. We conclude that the neglected corrections coming from inside of the wall contributions are indeed negligible for scalars.

2.7 Procedure for the momentum transfer calculation: summary

In this section we summarise the previous results and give a concise prescription for the momentum transfer calculation independent of the wall shape details. There are three contributions:

$$\langle \Delta p_L^{\text{step}} \rangle, \quad \langle \Delta p_R^{\text{step}} \rangle, \quad \langle \Delta p^{\text{wkb}} \rangle, \quad (45)$$

where the first two correspond to emission to the left and right in the step wall regime and the last one to the emission to the right in the WKB regime. These are given explicitly by the following phase space integrals:

$$\begin{aligned}
\langle \Delta p_L^{\text{step}} \rangle &= \int_0^{k_z^{\text{max}}} \frac{dk_z}{2\pi} \frac{1}{2k_0} \int_0^{k_{\perp, \text{max}}^2} \frac{dk_{\perp}^2}{4\pi} \cdot \frac{1}{2p^z} \left[\frac{1}{2|q^z|} |\mathcal{M}_L|^2 (p^z - q^z + k^z) \right] \Theta(L_w^{-1} - k^z) , \\
\langle \Delta p_R^{\text{step}} \rangle &= \int_{\Delta m}^{k_z^{\text{max}}} \frac{dk_z}{2\pi} \frac{1}{2k_0} \int_0^{k_{\perp, \text{max}}^2} \frac{dk_{\perp}^2}{4\pi} \cdot \frac{1}{2p^z} \left[\frac{1}{2|q^z|} |\mathcal{M}_R|^2 (p^z - q^z - \tilde{k}^z) \right] \Theta(L_w^{-1} - k^z) , \\
\langle \Delta p^{\text{wkb}} \rangle &= \int_{\Delta m}^{k_z^{\text{max}}} \frac{dk_z}{2\pi} \frac{1}{2k_0} \int_0^{k_{\perp, \text{max}}^2} \frac{dk_{\perp}^2}{4\pi} \cdot \frac{1}{2p^z} \left[\frac{1}{2|q^z|} |\mathcal{M}^{\text{wkb red.}}|^2 (p^z - q^z - \tilde{k}^z) \right] \\
&\quad \times \Theta(k^z - L_w^{-1}) \Theta(L_w^{-1} - (p^z - q^z - \tilde{k}^z)) , \tag{46}
\end{aligned}$$

where the limits $k_z^{\text{max}}, k_{\perp, \text{max}}^2$ were defined in eq. (34) but we repeat them here for the reader's convenience,

$$\begin{aligned}
k_z^{\text{max}} &\equiv \sqrt{(p_0 - m_{\psi})^2 - m^2} , \\
k_{\perp, \text{max}}^2 &\equiv \frac{1}{4p_0^2} (p_0^2 + k_z^2 + m^2 - m_{\psi}^2)^2 - k_z^2 - m^2 . \tag{47}
\end{aligned}$$

and also recall that $\Delta m^2 \equiv \tilde{m}^2 - m^2$. $\mathcal{M}_L, \mathcal{M}_R$ are the amplitudes for the process calculated using the step wall ansatz (see section 2.4) and $\mathcal{M}^{\text{wkb red.}}$ is the amplitude in the WKB approximation, without the contribution inside the wall, calculated following the discussion in section 2.6. Note the presence of various Theta functions imposing cuts on phase space. For the $\langle \Delta p_{L,R}^{\text{step}} \rangle$ cases, these ensure that $k^z < L_w^{-1}$, i.e. a step wall approximation is valid. Similarly $\Theta(k^z - L_w^{-1})$ for the WKB regime. For the latter, the second constraint $\Theta(L_w^{-1} - (p^z - q^z - \tilde{k}^z))$ imposes that the momentum transfer not surpass the inverse wall width (see discussion near eq. (39)). In practice, all constraints can be implemented by cutting the integration limits, as is shown in Table 1. The $\Theta(\pm(L_w^{-1} - k^z))$ are easily implemented by cutting the k^z integration appropriately. For the WKB regime, the extra constraint $p^z - q^z - \tilde{k}^z < L_w^{-1}$ amounts to cutting also the k_{\perp}^2 integration as follows

$$k_{\perp}^2 \leq \begin{cases} k_{\perp, \text{wkb}}^2 , & k^z < k_*^z \\ k_{\perp, \text{max}}^2 , & k^z > k_*^z \end{cases} \quad (\text{WKB red.}) \tag{48}$$

where

$$k_{\perp, \text{wkb}}^2 \equiv \frac{1}{4p_0^2} \left(p_0^2 + k_z^2 + m^2 - m_{\psi}^2 - (p^z - \tilde{k}^z - L_w^{-1})^2 \right)^2 - k_z^2 - m^2 , \tag{49}$$

$$k_*^z \equiv \sqrt{(p^z - L_w^{-1})^2 + \Delta m^2} . \tag{50}$$

To derive this, note that if $p^z - \tilde{k}^z - L_w^{-1} < 0$, the positivity of q^z means we are done with no extra condition. If instead $p^z - \tilde{k}^z - L_w^{-1} > 0$, squaring the constraint and solving for k_{\perp}^2 gives eq. (49).

Phase space integration limits				
	L -step	R -step	WKB red.	
k_z	$[0, \text{Min}[L_w^{-1}, k_{\text{max}}^z]]$	$[\Delta m, \text{Min}[L_w^{-1}, k_{\text{max}}^z]]$	$[L_w^{-1}, \text{Max}[L_w^{-1}, k_*^z]]$	$[\text{Max}[L_w^{-1}, k_*^z], k_{\text{max}}^z]$
k_{\perp}^2	$[0, k_{\perp, \text{max}}^2]$	$[0, k_{\perp, \text{max}}^2]$	$[0, k_{\perp, \text{wkb}}^2]$	$[0, k_{\perp, \text{max}}^2]$

Table 1: We report here all phase space integration limits for each emission contribution after explicitly taking into account constraints imposed by Theta functions in eq. (46). The WKB regime is divided into two regions having imposed the constraint $\Delta p_z L_w < 1$, as explained in section 2.7. All definitions Max & Min functions are included to also capture low p^0 or large L_w^{-1} .

2.8 Momentum transfer from scalar emission

Using the expressions summarised in section 2.7, we calculate the momentum transfer from scalar emission $\psi \rightarrow \psi\phi$ in our toy model eq. (5). As explained above, the total averaged momentum transfer is the sum of three separate contributions $\langle \Delta p_{L,R}^{\text{step}} \rangle$, $\langle \Delta p_R^{\text{wkb}} \rangle$. Numerical integration is relatively straightforward and representative results are shown in fig. 5. Analytical expressions can be derived, with some details given in appendix E.1, and are presented when deemed useful. There are several parameters in the problem so which of the three contributions dominates is a function of different hierarchies. Generically we find that at large energies $p^0 \rightarrow \infty$ the WKB contribution always dominates and falls off as $1/p^0$. Computing the phase space integrals in this asymptotic limit, we obtain a very good approximation

$$\langle \Delta p^{\text{total}} \rangle \Big|_{p_0 \gg L_w^{-1} \text{Max}[1, m_\psi/m]} \approx \langle \Delta p_R^{\text{wkb}} \rangle \approx \frac{y^2 \tilde{m}}{32\pi^2 m_\psi^2} \times \quad (51)$$

$$\frac{p_0^{-1}}{2\tilde{m}} \left[2\tilde{m}^2 \ln\left(\frac{m}{\tilde{m}}\right) + \frac{2(m^2 + \tilde{m}^2)m_\psi^2 - m^2\tilde{m}^2}{S(m)} \ln[D(m)] + S(\tilde{m}) \ln[D(\tilde{m})] \right],$$

where

$$D(m) \equiv \frac{m^2 - 2m_\psi^2 + S(m)}{2m_\psi^2}, \quad S(m) \equiv im\sqrt{4m_\psi^2 - m^2}.$$

On the other hand, at low and intermediate relativistic energies, the step function contributions typically dominate. This behaviour is amplified in two independent regimes. For very thin wall $L_w \rightarrow 0$ the WKB contribution naturally only turns on at higher energies $p_0 \gg L_w^{-1}$, with $\langle \Delta p_R^{\text{step}} \rangle$ temporarily dominating in its place (see bottom-right panel of fig. 5). Nonetheless, the trend is still reasonably approximated by interpolating backward the asymptotic result of eq. (51).

More interesting is the case when the initial mass of ϕ is very light $m \ll \tilde{m}, m_\psi$. Each contribution to momentum transfer becomes constant for an inter-relativistic plateau as can be observed in the leftmost panel of fig. 5. Moreover, it is actually

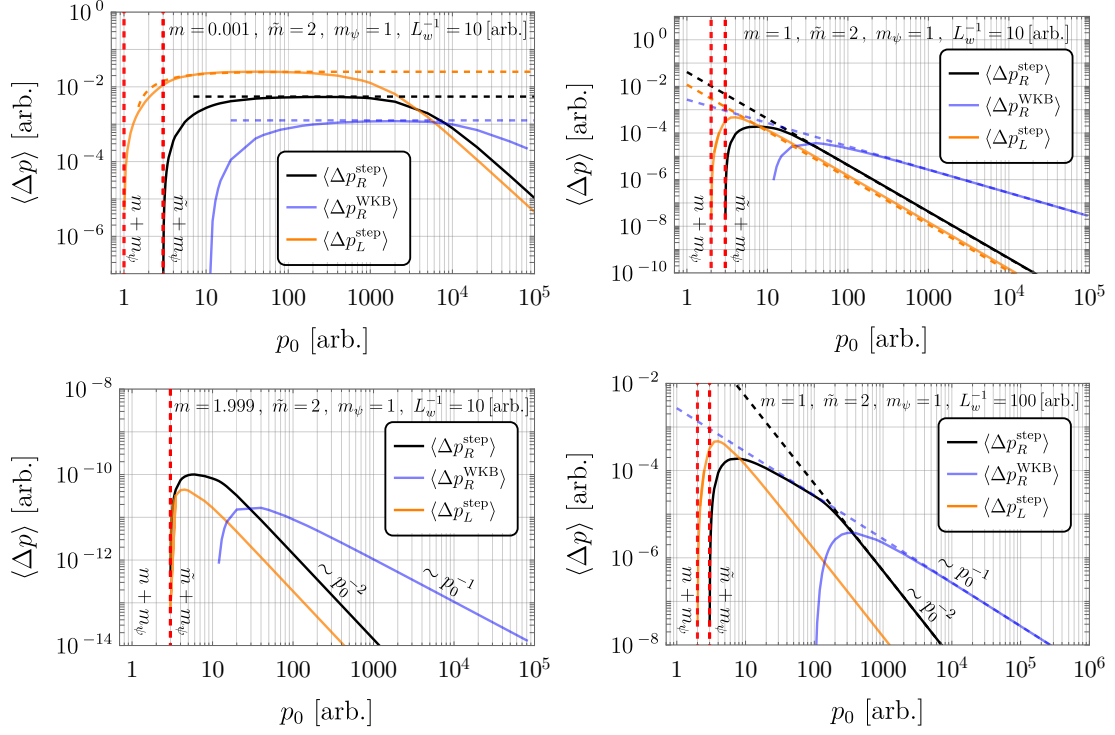


Figure 5: Numerical results for the averaged momentum transfer to the wall for each of the three contributions in eq. (46) as a function of incoming particle energy. Black and orange curves stand for right and left emission of soft quanta (using step wall), while blue is for the energetic quanta (using WKB). The vertical red dashed lines are the lower bounds on the minimal energy the incoming particle can have to emit right and left modes. We show four cases of interest, that respectively are: $\tilde{m} \gg m$, $\tilde{m} \sim O(1)m$, $\tilde{m} - m \ll 1$ and $L_w^{-1} \gg \tilde{m}$. The horizontal and oblique dashed lines are analytical estimates in eq. (51) ($\langle \Delta p_{\zeta_R}^{\text{wkb}} \rangle$), in eq. (197) ($\langle \Delta p_{\zeta_L}^{\text{step}} \rangle$) and in eq. (198) ($\langle \Delta p_{\zeta_R}^{\text{step}} \rangle$). At the highest scales, the WKB contribution always dominates and falls as p_0^{-1} (while both step wall contributions fall as p_0^{-2}). In the limit $L_w \rightarrow 0$, R emission also falls off as p_0^{-1} . Most interestingly, for large hierarchy m_ψ/m , $\langle \Delta p \rangle$ is constant until $p_0 \lesssim \tilde{m}m_\psi/m$.

$\langle \Delta p_L^{\text{step}} \rangle$ that dominates, with a value

$$\langle \Delta p^{\text{total}} \rangle \approx \langle \Delta p_L^{\text{step}} \rangle \approx \frac{y^2 \tilde{m}}{8\pi^2 m_\psi^2} \quad \text{for } p_0 \lesssim \tilde{m}m_\psi/m. \quad (52)$$

Further details can be found in appendix E.1.

2.9 Pressure from scalar emission

The pressure induced on the bubble wall from scalar emission is finally obtained by integrating over the incoming flux

$$\mathcal{P} = \int \frac{d^3 p}{(2\pi)^3} f_\psi(T, \gamma_w) \times \frac{p^z}{p_0} \langle \Delta p^{\text{total}} \rangle, \quad (53)$$

where f_ψ is the phase space distribution of incoming ψ particles in the frame of the wall. Let us first focus on the interesting regime when $m \ll m_\psi$, identified in eq. (52), where $\langle \Delta p \rangle^{\text{total}}$ is constant for a plateau lasting till $p_0 \lesssim \tilde{m}m_\psi/m$. In the ultra-relativistic limit $p^z/p_0 \rightarrow 1$, and the integration gives simply

$$\mathcal{P}^{\text{scalar}} = n_\psi(T, \gamma_w) \langle \Delta p^{\text{total}} \rangle = \gamma_w n_\psi(T) \langle \Delta p^{\text{total}} \rangle, \quad p_0 \lesssim \frac{\tilde{m}m_\psi}{m}. \quad (54)$$

To go from the second equality to the third we used that the number density of ψ in the wall frame is boosted with respect to the FRW frame number density. Thus, even scalar emission can cause friction pressure that grows with γ_w . Combining the plateau and asymptotic contributions for scalar emission, we have approximately, for an incident thermal population,

$$\mathcal{P}^{\text{scalar}} \approx \begin{cases} \frac{T^3}{8\pi^4} \frac{y^2 \tilde{m}}{m_\psi^2} \times \gamma_w, & \gamma_w \lesssim \frac{\tilde{m}m_\psi}{mT} \\ \frac{T^2}{64\pi^3} \frac{y^2 \tilde{m}^2}{m_\psi m}, & \gamma_w \gtrsim \frac{\tilde{m}m_\psi}{mT} \end{cases}, \quad (55)$$

where the second expression was obtained by expanding eq. (51) for small m and simply multiplying by $n_\psi(T) \approx T^3/\pi^2$. The asymptotic constant pressure can be compared with the LO contribution from a thermal population of ϕ particles crossing the wall as per eq. (1), which gives $\sim T^2 \tilde{m}^2$. We observe that the NLO contribution is more important when $\frac{y^2}{64\pi m_\psi m} \gtrsim 1$.

We remind the reader that our results for scalar emission pressure were obtained for a particularly simple choice of interactions in the Lagrangian eq. (5) (with $y = \text{const}$) and we highlighted here a particular regime of parameters. Our main goal was to mimic as much as possible the vector radiation to be discussed in the next section. We will return to whether the pressure in eq. (55) can be phenomenologically relevant in future work.

3 Spontaneously broken gauge theories

We now proceed to the phase transitions related to the spontaneous breaking of gauge symmetry and the emission of vector bosons. The procedure will in essence be exactly the same as what we presented for the case of the scalar emission. We will quantise the theory of a gauge field in the background of a domain wall interpolating between a symmetric and broken phase. As should be expected, the extra difficulty will involve dealing with gauge-fixing, spin and the change of degrees of freedom due to the spatially-dependent rearrangement of the vacuum.

For simplicity, we will consider the Abelian Higgs model of a charged complex scalar H , whose potential $V(\sqrt{2}|H|)$ is responsible for the spontaneous breaking of the $U(1)$ gauge symmetry. A second scalar field ψ charged under the same $U(1)$ will play the role of matter; its potential is trivial. The Lagrangian is

$$\mathcal{L} = -\frac{1}{4} F_{\mu\nu} F^{\mu\nu} + |D_\mu H|^2 - V(\sqrt{2}|H|) + |D_\mu \psi|^2 - m_\psi^2 |\psi|^2, \quad (56)$$

where we are using the convention $D_\mu \psi = (\partial_\mu + igA_\mu)\psi$ and A_μ is the vector gauge field. We will in general not need to commit to a specific potential but will simply

assume that it has two minima at $\sqrt{2}|H| = v, \tilde{v}$, where $v \rightarrow 0$ corresponds to the symmetric phase. We will quantise the theory in the background of a domain wall $\sqrt{2}\langle |H| \rangle = v(z)$. We will also be interested, both as a computational tool and as a phenomenological case in its own right, in imagining a distorted or more general class of potential with non-zero $v < \tilde{v}$. We will call this scenario a *broken to broken* phase transition, in opposition to the more familiar case of *symmetric to broken* phase transitions.

To work with the theory described by eq. (56), one has to make two independent choices: what field coordinates to use for H , such as Cartesian or polar, and what gauge to impose. The value of each choice is determined by the particular application. Much of the following pages will be dedicated to arguing for the most convenient choices for our application.

If we are interested in studying the geometry of the vacuum manifold, polar coordinates $H = \frac{1}{\sqrt{2}}(h + v)e^{i\theta}$ are most convenient. The potential depends only on the modulus. In the symmetric phase however, this coordinate choice is singular. On the other hand, Cartesian coordinates are well-defined everywhere

$$H = \frac{1}{\sqrt{2}}(h_1 + ih_2) \equiv \frac{1}{\sqrt{2}}(h + v(z) + ih_2) \ , \quad (57)$$

where we have expanded around the background solution $h_1 = v(z)$. The Lagrangian for the Higgs and gauge fields becomes

$$\begin{aligned} \mathcal{L}_{A,H} = & -\frac{1}{4}F_{\mu\nu}F^{\mu\nu} + \frac{1}{2}(\partial h)^2 + \frac{1}{2}(\partial h_2)^2 - gA^\mu [h_2\partial_\mu v(z) - v(z)\partial_\mu h_2] \\ & + \frac{1}{2}g^2v^2(z)A^2 - \frac{1}{2}\partial_1^2V(v(z))h^2 - \frac{1}{2}\partial_2^2V(v(z))h_2^2 + \dots \ , \end{aligned} \quad (58)$$

up to quadratic terms, where $\partial_i \equiv \partial/\partial h_i$, so that the last two terms are the z -dependent mass terms of h and h_2 .

At a non-zero minimum of the potential, h_2 becomes massless and is the would-be Nambu-Goldstone boson (NGB). As always for gauge theories, when $v \neq 0$ a mixing term appears between this goldstone boson and the gauge boson. However, in the context of a varying background, there is also an extra mixing proportional to $\partial_z v$. When v is a constant, the mixing can be eliminated completely while also gauge fixing by adding the so called R_ξ gauge term

$$\delta\mathcal{L}_{g.f.} = -\frac{1}{2\xi}(\partial_\mu A^\mu - \xi g v h_2)^2 \ , \quad (59)$$

and integrating by parts. For $v = v(z)$, adding this same (now z -dependent) gauge-fixing term does not get rid of mixing entirely but localises it to the region of the wall

$$\begin{aligned} \mathcal{L}_{A,H} + \delta\mathcal{L}_{g.f.} = & -\frac{1}{4}F_{\mu\nu}F^{\mu\nu} - \frac{1}{2\xi}(\partial_\mu A^\mu)^2 + \frac{1}{2}(\partial h)^2 + \frac{1}{2}(\partial h_2)^2 \\ & - 2gh_2A^z\partial_z v(z) + \frac{1}{2}g^2v(z)^2A^2 - \frac{1}{2}\partial_1^2V(v(z))h^2 \\ & - \frac{1}{2}[\partial_2^2V(v(z)) + \xi g^2v^2(z)]h_2^2 + \dots \ . \end{aligned} \quad (60)$$

3.1 Particle content in the asymptotic regions

We briefly remind ourselves of the spectrum of the theory in the asymptotic regions $v = 0$ and \tilde{v} at $z \rightarrow -\infty$ and $z \rightarrow \infty$ respectively, before discussing the full interpolating space.

Symmetric phase: The theory eq. (60) around the symmetric point minimum $v = 0$ describes two scalars $h_{1,2}$, with equal mass by symmetry

$$m_{h,s}^2 \equiv \partial_1^2 V(0) = \partial_2^2 V(0) \quad (61)$$

The gauge-fixing affects only the Maxwell equations of motion for the massless vector A^μ . Whatever the value of ξ , we can identify two physical transverse (in the sense that $A_\mu k^\mu = 0$) degrees of freedom with polarisation vectors given by

$$\epsilon_{T_1}^\mu = (0, 0, 1, 0) , \quad \epsilon_{T_2}^\mu = \frac{1}{\sqrt{k_\perp^2 + k_z^2}}(0, k^z, 0, -k_\perp) , \quad (62)$$

for $k^\mu = (k_0, k_\perp, 0, k^z)$. The only (well-known) subtlety involves imposing on the Hilbert space a constraint to project out unphysical states, the so-called Gupta-Bleuler condition [73].

Broken phase(s): At a symmetry breaking minimum $\partial_2^2 V(\tilde{v}) = 0$ and h_2 describes the would-be NGB. A particularly convenient choice is ‘unitary gauge’, corresponding to $\xi \rightarrow \infty$ in which the NGB decouples completely, making manifest the spectrum. We are left with a single massive scalar (the Higgs) h with mass squared equal to $\partial_1^2 V(\tilde{v})$ and a massive vector boson A_μ with mass

$$\tilde{m} \equiv g\tilde{v} , \quad (63)$$

and satisfying the Proca equation

$$\partial_\mu F^{\mu\nu} + \tilde{m}^2 A^\nu = 0 . \quad (64)$$

This reduces to a Klein-Gordon equation for each component of A^μ supplemented by the Lorentz condition:

$$\implies \partial^2 A^\mu + \tilde{m}^2 A^\mu = 0 , \quad \partial_\mu A^\mu = 0 . \quad (65)$$

Solving this is straightforward and one adds to the transverse polarisations of eq. (62) a third longitudinal one parallel to 3-momentum

$$\epsilon_L^\mu = \left(\frac{k_0^2 - m^2}{k_0}, k_\perp, 0, k^z \right) \frac{k_0}{m\sqrt{k_0^2 - m^2}} . \quad (66)$$

3.2 Global degrees of freedom

Here will analyse the fields defined over the entire region and identify the appropriate global modes to quantise, where by global we simply mean they are good across the wall.

In principle, one could choose a convenient value of ξ in eq. (60) and push ahead with quantisation. However, we would have to deal with mixing when solving for the mode functions, as well as taking care to impose a non-trivial Gupta-Bleuler like condition on physical states. Luckily, we will argue that even when asymptotically approaching the symmetric point as $z \rightarrow -\infty$, it is possible to work with unitary gauge $\xi \rightarrow \infty$ with impunity. This approach was already made at the classical level in ref. [70], and we will re-derive and tweak some of their results using a slightly different language, before quantising.

In unitary gauge, the h_2 degree of freedom decouples and the theory becomes

$$\mathcal{L}_{A,H}^{U.G.} = -\frac{1}{4}F_{\mu\nu}F^{\mu\nu} + \frac{1}{2}g^2v^2(z)A^2 + \frac{1}{2}(\partial h)^2 - \frac{1}{2}\partial_1^2V(v)h^2 + \dots, \quad (67)$$

and the equations of motion for eq. (58) reduce to just two uncoupled equations

$$\square h = -V''(v)h, \quad (68)$$

$$\partial_\nu F^{\mu\nu} = g^2v^2(z)A^\mu. \quad (69)$$

The first one is the equation of motion for the physical Higgs boson h and we will not have any more to say about it here. The second will be the focus of our attention. While $v(z) > 0$, the theory is always in a broken phase and A^μ describes a massive vector. Unitary gauge is then manifestly a valid choice. Note that the usual transversality condition for massive vector bosons in this case becomes

$$\partial_\mu \partial_\nu F^{\mu\nu} = \partial_\mu (g^2v^2 A^\mu) = 0, \quad (70)$$

$$\implies \partial_n A^n + \partial_z A^z = -\frac{\partial_z v^2}{v^2} A^z, \quad (71)$$

which, in the presence of the domain wall, generalises the standard Lorentz condition for massive electrodynamics in eq. (65). The constraint above ensures this vector field has three polarisation degrees of freedom. Subbing this back into eq. (69) we get

$$\partial^2 A^\mu + \partial^\mu \left[\left(\frac{\partial_z v^2}{v^2} \right) A^z \right] + g^2v^2 A^\mu = 0. \quad (72)$$

The general Fourier mode can be written as

$$A_{k_0, k_\perp}^\mu = e^{-ik_n x^n} \sum_l a_l \chi_{l, k_n}^\mu(z), \quad (73)$$

where l runs over three indices, a_l are some constant Fourier coefficients and the functions $\chi_{l, k_0, k_\perp}^\mu(z)$ have to be found by solving eq. (72). One might be tempted to define left and right moving χ^μ modes by fixing the incoming piece at infinity in terms of conventional transverse and longitudinal modes eqs. (62) and (66). However, under such a choice, transmitted and reflected pieces would contain also other polarisations. Fundamentally, this is because for non-zero k_\perp , rotations around \vec{k} are not a symmetry and conventional spin is not conserved. We now construct more convenient ‘wall polarisations’, which instead do not mix.

τ polarisations: It is useful to define what we call τ -polarisations by the condition $A^z = 0$, since for these we recover the Lorentz condition $\partial_\mu A^\mu = 0$, which in Fourier space reduces to

$$k_n \chi_\tau^n \equiv k_0 \chi_\tau^0 - k_\perp \chi_\tau^\perp = 0, \quad (74)$$

and has solutions in terms of two *constant* vectors

$$\chi_\tau^\mu = \epsilon_{\tau_{1,2}}^\mu \chi_{\tau_{1,2}}(z), \quad (75)$$

where

$$\epsilon_{\tau_1}^\mu = (0, 0, 1, 0), \quad \epsilon_{\tau_2}^\mu = (k_\perp, k_0, 0, 0) / \sqrt{k_0^2 - k_\perp^2}, \quad (76)$$

and the equations of motion eq. (72) become the Klein-Gordon-like

$$[-E^2 - \partial_z^2 + g^2 v^2(z)] \chi_{\tau_{1,2}}(z) = 0, \quad (77)$$

where we remind the reader of the definition $E = \sqrt{k_0^2 - k_\perp^2}$. Note that $\epsilon_{\tau_1}^\mu$ is one of the standard transverse polarisations, but $\epsilon_{\tau_2}^\mu$ is not, since it has a non-zero time component, and is not orthogonal to three momentum. The wave equation to solve across the wall for τ d.o.f. is thus identical to the scalar case studied in section 2.

λ polarisation: It remains to solve for the remaining degree of freedom with $A^z \neq 0$. The wave equation to solve for is obtained by setting $\mu = z$ in eq. (72). We note already that it is significantly more complicated than what we found for τ . Whatever the solution for A^z , the other components of the vector are fixed. Requiring orthogonality with χ_τ^μ implies the form $\chi_\lambda^\mu(z) = (-ik^n \alpha(z), \chi_\lambda^z)$ where we recall $n = 0, \perp$. The generalised Lorentz condition in eq. (71) immediately leads to the relation

$$\alpha(z) = \frac{\partial_z (v^2 \chi_\lambda^z)}{E^2 v^2}. \quad (78)$$

Plugging this back into the eq. (72), we obtain the equation in terms of the χ^z only

$$-E^2 \chi_\lambda^z - \partial_z \left(\frac{1}{v^2} \partial_z (v^2 \chi_\lambda^z) \right) + g^2 v^2(z) \chi_\lambda^z = 0. \quad (79)$$

We can get rid of the linear in derivative term if we introduce a new function $\lambda(z)$

$$\chi_\lambda^z = \frac{E}{g v(z)} \lambda(z), \quad (80)$$

and eq. (79) becomes Schrodinger-like

$$(-E^2 - \partial_z^2 + U_\lambda(z)) \lambda = 0, \quad (81)$$

with effective potential

$$\begin{aligned}
U_\lambda(z) &= g^2 v^2(z) - v \partial_z \left(\frac{\partial_z v}{v^2} \right) \\
&= g^2 v^2(z) + 2 \left(\frac{\partial_z v}{v} \right)^2 - \frac{\partial_z^2 v}{v} .
\end{aligned} \tag{82}$$

The solutions in terms of λ , unlike χ_λ^z , satisfy the usual orthogonality relations

$$\int dz \lambda_k(z) \lambda_q^*(z) = 2\pi \delta(k^z - q^z) . \tag{83}$$

It is easy to prove – and we do so explicitly in appendix D – that for an interpolating solution $v(z)$ of a completely arbitrary Higgs potential V , we have $(v'/v)^2, v''/v \rightarrow m_{h,s}^2$ as $z \rightarrow -\infty$ so that $U_\lambda(z)$ is always finite even if $v = 0$. More precisely

$$\lim_{z \rightarrow -\infty} U_\lambda(z) = \begin{cases} g^2 v^2 , & v \neq 0 \\ m_{h,s}^2 , & v = 0 \end{cases} \equiv m_\lambda^2 . \tag{84}$$

We see that λ is the perfect cross-wall field. It interpolates between one of the massive (Higgs) degrees of freedom on the symmetric $v = 0$ side $z \rightarrow -\infty$ and a third component of the massive vector in the broken region $z \rightarrow \infty$. If instead $v \neq 0$, λ simply interpolates between the different mass vectors.

Let us look more closely at the A^μ vector formed by the λ field. Using the equations of motion forces the on-shell relation:

$$\begin{aligned}
\chi_\lambda^z &= \frac{E^2 \partial_z \alpha}{E^2 - g^2 v^2(z)} \Rightarrow \\
\chi_\lambda^\mu &= (-ik^n \alpha(z), \chi_\lambda^z) = (-ik^n, \partial^z) \alpha(z) + \frac{g^2 v^2(z)}{E^2} \chi_\lambda^z(0, 0, 0, 1) \\
&= (-ik^n, \partial^z) \alpha(z) + \frac{gv(z)}{E} \lambda(z)(0, 0, 0, 1)
\end{aligned} \tag{85}$$

So that the vector can be written as a total derivative plus a term sub-leading in energy. This form will turn out to be very useful in calculating the amplitudes for physical processes. Far from the wall, when $v \rightarrow const$, we can introduce the polarisation vector ϵ_λ^μ such that

$$\begin{aligned}
\chi_\lambda^\mu &\propto \epsilon_\lambda^\mu, \quad \epsilon_\mu^\lambda \epsilon^{\lambda\mu} = -1 \\
\epsilon_\lambda^\mu &= \left(k^n \frac{k^z}{E^2}, 1 \right) \times \frac{E}{gv} \\
&= \frac{k^z}{Egv} k^\mu + \frac{gv}{E} (0, 0, 0, 1) .
\end{aligned} \tag{86}$$

We emphasise again that these λ and τ differ from the conventional transverse and longitudinal polarisations. Far from the wall, all polarisations satisfy the same equation of motion and one can use any linear combination of either basis to decompose

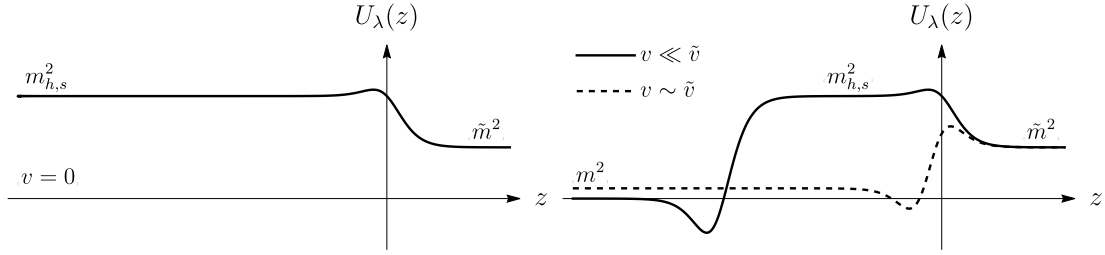


Figure 6: The potential for the λ degree of freedom, which is defined everywhere. Recall $m = gv$ and $\tilde{m} = g\tilde{v}$, plus thermal corrections. As $v \rightarrow 0$ a growing plateau develops ending at $z \sim m_{h,s}^{-1} \ln(v/\tilde{v})$ with value $m_{h,s}^2$ - the symmetric side mass of the Higgs in the case $v = 0$ exactly. These curves were drawn using the explicit profile eq. (93).

the vector field. We can relate the wall polarisations to the conventional longitudinal and transverse ones in eqs. (62) and (66) via the rotation matrix

$$\begin{pmatrix} \epsilon_{T_1} \\ \epsilon_{T_2} \\ \epsilon_L \end{pmatrix} = \begin{pmatrix} 1 & 0 & 0 \\ 0 & \frac{k_0 k^z}{E\sqrt{k_0^2 - m^2}} & -\frac{k_\perp m}{E\sqrt{k_0^2 - m^2}} \\ 0 & \frac{k_\perp m}{E\sqrt{k_0^2 - m^2}} & \frac{k_0 k^z}{E\sqrt{k_0^2 - m^2}} \end{pmatrix} \begin{pmatrix} \epsilon_{\tau_1} \\ \epsilon_{\tau_2} \\ \epsilon_\lambda \end{pmatrix}. \quad (87)$$

In the case of a very large k^z , $E \gg k_\perp, m$ the mixing angle between τ, λ transverse and longitudinal scales as m/E . We can see that the two bases of polarisations are exactly the same for the case $k_\perp = 0$. This is expected since for this configuration of momenta T_1, T_2 polarisations have zero components in the z direction. Using the unbroken part of the Lorentz symmetry (boosts in $x - y$ direction) we can obtain the polarisations for generic momenta, which indeed agrees with the τ, λ basis derived before. Our goal in this paper is to calculate the total pressure acting on the domain wall and for this, we sum the contributions from all polarisations. We perform all of the calculations in the τ, λ basis, without even reporting the results for T, L polarisations.

3.2.1 $v \rightarrow 0$ limit

All of the previous discussion applied most manifestly for the case when the vev of the symmetry breaking field is $v \neq 0$. What happens in the case when the domain wall on one side approaches a vacuum where the gauge symmetry is unbroken? We saw in the previous section that the potential of the λ mode has a property that as $v \rightarrow 0$ then $U_\lambda(z) \rightarrow m_{h,s}^2$, which together with our expectations from the Higgs phenomena hints that on the unbroken side λ should correspond to the would-be NGB

$$\lambda_{z \rightarrow -\infty} \rightarrow h_2. \quad (88)$$

To understand this matching better, let us look at the χ_λ^μ vector in the limit $v \rightarrow 0$

$$\begin{aligned}\chi_\lambda^\mu &= (-ik^n \alpha(z), \chi_\lambda^z) = \left(\frac{-ik^n \partial_z(v\lambda)}{gEv^2}, \frac{E}{gv} \lambda \right) \\ &= \frac{\lambda}{gv} \left(-\frac{ik^n}{E} \left[\frac{v'}{v} + \frac{\lambda'}{\lambda} \right], E \right) \Big|_{v \rightarrow 0} = \frac{e^{-ikx}}{gv} \left(\frac{k^n}{E} [-im_{h,s} + k^z], E \right),\end{aligned}\quad (89)$$

where we have used that λ becomes a plane wave far from the wall and $v'/v \rightarrow m_{h,s}$. Note that the factor $(-im_{h,s} + k^z)/E$ is a pure phase if the λ dof is on shell. Let us see whether we can build exactly the same vector but from the field h_2 . Indeed if we consider the vector

$$\partial^\mu \left(\frac{h_2}{gv} \right) = -\frac{e^{-ikx}}{gv} \left(k^n, k^z + i \frac{v'}{v} \right) = \frac{-iEe^{-ikx}}{gv(k^z - im_{h,s})} \left(\frac{k^n}{E} [-im_{h,s} + k^z], E \right). \quad (90)$$

So we can see, comparing with eq. (89), that the two vectors χ_λ^μ and $\partial_\mu(h_2/gv)$ are exactly the same apart from the constant phase factor, so indeed λ field in the $z \rightarrow -\infty$ limit corresponds to the Goldstone boson.

What about starting from a finite value and taking $v \rightarrow 0$? For concreteness let us consider the potential

$$V = \lambda_h (|h| - v)^2 (|h| - \tilde{v})^2. \quad (91)$$

First of all the potential has a cusp at $|h| = 0$ so the limit $v \rightarrow 0$ becomes discontinuous. This can be seen also in the form of $U_\lambda(z)$. As v becomes smaller a longer finite plateau develops in the potential with value $\approx m_{h,s}^2$, as is shown in fig. 6. No matter how small v eventually the potential turns down and asymptotes to g^2v^2 as is to be expected. Thus for any finite though tiny v the asymptotic states at $z \rightarrow -\infty$ are those of a massive vector.

3.3 The step wall case

In order to proceed further we need to solve the equations of motion. In general, it is a complicated problem depending on the shape of the effective potential $V_{\text{eff}}(h)$ at the time of the phase transition. One needs to find the solitonic solution $v(z)$ connecting false and true vacuum and later the wavemodes describing perturbations of each field on this background. In the particular case of the domain wall

$$v(z) = \frac{1}{2} \tilde{v} \left(1 + \tanh \left(\frac{z}{L_w} \right) \right), \quad (92)$$

solutions were found in [70] in terms of hypergeometric functions. In this paper, we will consider an even simpler case, namely a step function ansatz for the wall. This approximation will of course be valid only if the momentum of the particle during the passage is (much) less than the inverse width of the wall $k, \tilde{k} \ll L_w^{-1}$. Typically, this width is controlled by the mass of the Higgs $L_w^{-1} \approx m_h$.

The solution of the equations of motion can be written down on each side immediately and the only challenge becomes deriving and implementing matching

conditions. In this section, we report the matching conditions for τ and λ polarisations and write down the corresponding wave functions. We will do so first for the broken to broken case $v > 0$. As an explicit example, we can imagine distorting eq. (92) to

$$v(z) \rightarrow v + \frac{1}{2}(\tilde{v} - v) \left(1 + \tanh \left(\frac{z}{L_w} \right) \right). \quad (93)$$

We then comment on the $v \rightarrow 0$ limit, which is straightforward for τ degrees of freedom but more delicate for λ .

3.3.1 (τ) polarisations

For the τ polarisations, we showed in section 3.2 that the equations of motion are exactly the same as for the scalar field ($\square A_{(\tau)}^\mu = -g^2 v^2 A_{(\tau)}^\mu$) and so for the step wall the matching conditions become:

$$\chi_{\tau_i}|_{<0} = \chi_{\tau_i}|_{>0}, \quad (94)$$

$$\partial_z \chi_{\tau_i}|_{<0} = \partial_z \chi_{\tau_i}|_{>0}, \quad (95)$$

with $i = 1, 2$. The reflection and transmission coefficients are thus the same as for scalars and the wave functions become

$$\chi_{\tau_i, R, k}^\mu(z) = e_{\tau_i}^\mu \begin{cases} e^{ik^z z} + r_k^\tau e^{-ik^z z}, & z < 0 \\ t_k^\tau e^{i\tilde{k}^z z}, & z > 0 \end{cases}, \quad (96)$$

$$\chi_{\tau_i, L, k}^\mu(z) = e_{\tau_i}^\mu \sqrt{\frac{k^z}{\tilde{k}^z}} \begin{cases} \frac{\tilde{k}^z}{k^z} t_k^\tau e^{-ik^z z}, & z < 0 \\ e^{-i\tilde{k}^z z} - r_k^\tau e^{i\tilde{k}^z z}, & z > 0 \end{cases}, \quad (97)$$

where

$$r_k^\tau = \frac{k^z - \tilde{k}^z}{k^z + \tilde{k}^z}, \quad t_k^\tau = \frac{2k^z}{k^z + \tilde{k}^z}, \quad (98)$$

$$k_0 = \sqrt{k_z^2 + m_\tau^2 + k_\perp^2}, \quad \tilde{k}^z = \sqrt{k_0^2 - \tilde{m}_\tau^2 - k_\perp^2}, \quad m_\tau \equiv gv, \quad \tilde{m}_\tau \equiv g\tilde{v}.$$

Taking the $v \rightarrow 0$ limit for these degrees of freedom is simple and we approach the $v = 0$ case smoothly.

3.3.2 (λ) polarisation

The λ modes require more work. Again we first focus on the broken to broken case of $v > 0$. Matching conditions are easy to derive by integrating the wave equation for λ once and twice respectively (most easily done at the level of eq. (79)). These are

$$\begin{aligned} \frac{\partial_z \lambda}{v(z)} \Big|_{<0} &= \frac{\partial_z \lambda}{v(z)} \Big|_{>0}, \\ v(z) \lambda \Big|_{<0} &= v(z) \lambda \Big|_{>0}, \end{aligned} \quad (99)$$

which allows us to write down the expressions for (in-state) ‘left’ and ‘right’ movers:

$$\lambda_{R,k}(z) = \begin{cases} e^{ik^z z} + r_k^\lambda e^{-ik^z z} , & z < 0 \\ t_k^\lambda e^{i\tilde{k}^z z} , & z > 0 \end{cases} \quad (100)$$

$$\lambda_{L,k}(z) = \sqrt{\frac{k^z}{\tilde{k}^z}} \begin{cases} \frac{\tilde{k}^z}{k^z} t_k^\lambda e^{-ik^z z} , & z < 0 \\ e^{-i\tilde{k}^z z} - r_k^\lambda e^{i\tilde{k}^z z} , & z > 0 \end{cases} \quad (101)$$

where

$$r_k^\lambda = \frac{\tilde{v}^2 k^z - v^2 \tilde{k}^z}{\tilde{v}^2 k^z + v^2 \tilde{k}^z} , \quad t_k^\lambda = \frac{2k^z v \tilde{v}}{\tilde{v}^2 k^z + v^2 \tilde{k}^z} , \quad (102)$$

$$k_0 = \sqrt{k_z^2 + m_\lambda^2 + k_\perp^2} , \quad \tilde{k}^z = \sqrt{k_0^2 - \tilde{m}_\lambda^2 - k_\perp^2} , \quad m_\lambda \equiv gv , \quad \tilde{m}_\lambda \equiv g\tilde{v} .$$

Notice that in the relativistic limit

$$r_k^\lambda \rightarrow \frac{\tilde{v}^2 - v^2}{\tilde{v}^2 + v^2} , \quad \text{for } k^z \gg m_\lambda, \tilde{m}_\lambda . \quad (103)$$

so that λ maintains a finite reflection probability as long as the step function is a valid approximation, as was pointed out in [68].

Interestingly we can see that $r_k^\lambda \rightarrow 1$ in the limit $v \rightarrow 0$, i.e. the wall becomes completely non-transparent for the λ polarisations in this limit. This in-penetrability of the wall deserves some discussion. Consider the explicit form of $U_\lambda(z)$ for the case of the *tanh* profile in eq. (93). As mentioned in section 3.2.1 and sketched in fig. 6, in the limit of $v \rightarrow 0$, $U_\lambda(z)$ develops a growing plateau with a height $\approx L_w^{-2} \sim m_{h,s}^2$ and width $L_{\text{plateau}} \sim L_w \log \tilde{v}/v$. In the step function approximation, the first scale is effectively treated as infinite. For $v = 0$ exactly, since $m_\lambda(-\infty) = m_{h,s}$, obviously there are no oscillating $\lambda_{R,k}$ modes at all in the step regime, while $\lambda_{L,k}$ are completely reflected. For v tiny but non-zero the potential *eventually* does instead relax to $m_\lambda^2 = g^2 v^2$ and both oscillating $\lambda_{L,R}$ solutions exist, though strongly constrained to live on opposite sides of the wall¹⁵: $|r_k| = 1 - \mathcal{O}(v^2/\tilde{v}^2)$. Back to the $v = 0$ exact case, one can also consider theories in which the two scales L_w and $m_{h,s}$ are decoupled (e.g. set $m_{h,s} = 0$ as an extreme case). Then again oscillating $\lambda_{L,R}$ modes will exist on both sides of the wall even as $L_w \rightarrow 0$. Still, by numerical inspection, we find total reflection ($|r_k| \rightarrow 1$) in the step wall limit, though we leave a proper proof to future work.

In conclusion, calculations in the step function regime for the symmetric to broken transition case ($v = 0$) can be computed starting from the $v \neq 0$ case, using wavemodes eqs. (100) and (101), and then finally setting $v \rightarrow 0$ in the amplitude at the end. Notice instead that the asymptotic masses in the phase space kinematics will need to be discontinuously changed from gv to $m_{h,s}$.

¹⁵One might question the validity of the step wall approximation for $k^z \gtrsim L_w^{-1}$ when the potential function $U_\lambda(z)$ has a very long plateau $v \ll \tilde{v}$. However, the solutions eqs. (100) and (101) capture exactly the qualitative behaviour described.

A comment on bound states: We have so far considered ‘scattering state’ solutions to the equations of motion, i.e. those which are plane waves far from the wall. What about bound states? In principle, such states are possible for λ polarisation. Ref [70] found the existence of one for the case $v = 0$ when the potential satisfies some specific constraints. The form of the potential for $v > 0$, for example, as sketched in fig. 6, suggests that a bound state might generically appear. The mass of these bound states is controlled by the scale L_w^{-1} , as is obvious by its absence in the step wall limit. One could in principle calculate in the WKB limit the amplitude for an incoming particle to excite this bound state. We leave this interesting exercise to future work.

3.4 Quantisation

Following on from the previous sections, we can expand the field into a complete basis of eigenmodes of the free theory in the background vev $v(z)$,

$$\begin{aligned} A^\mu &= \sum_{I,\ell} \int \frac{d^3k}{(2\pi)^3 \sqrt{2k_0}} \left(a_{\ell,I,k}^{\text{in}} e^{-i(k_0 t - \vec{k}_\perp \cdot \vec{x})} \chi_{\ell,I,k}^\mu(z) + h.c. \right) \\ &= \sum_{I,\ell} \int \frac{d^3k}{(2\pi)^3 \sqrt{2k_0}} \left(a_{\ell,I,k}^{\text{out}} e^{-i(k_0 t - \vec{k}_\perp \cdot \vec{x})} \zeta_{\ell,I,k}^\mu(z) + h.c. \right), \end{aligned} \quad (104)$$

where $I = R, L$ denote right and left movers, $\ell = \tau_1, \tau_2$, λ sums over different wall polarisations. The wave modes $\chi^\mu(z)$ are in general constructed via

$$\chi_{\tau_i,I,k}^\mu = \epsilon_{\tau_i}^\mu \chi_{\tau_i,I,k}(z), \quad (105)$$

$$\chi_{\lambda,I,k}^\mu = \left(\frac{-ik^n \partial_z (v \lambda_{I,k})}{gE v^2}, \frac{E}{g v} \lambda_{I,k} \right) \stackrel{\text{on shell}}{=} \bar{\partial}^\mu \left(\frac{\partial_z (v \lambda_{I,k}^z)}{E g v^2} \right) + \frac{g v(z)}{E} \lambda_{I,k} \delta_z^\mu, \quad (106)$$

where $\bar{\partial}^\mu \equiv (-ik^n, \partial^z)$, with the explicit form of scalar fields $\chi_{\tau_i,I,k}(z)$ and $\lambda_{I,k}(z)$ obtained by solving the respective Schrodinger-like wave eqs. (77) and (81) with appropriate R, L -mover boundary conditions. In the step wall approximation for the vev $v(z)$, these are given analytically in eqs. (96), (97), (100) and (101). In complete analogy to the case of fundamental scalars¹⁶, the modes $\chi_{\ell,I,k}^\mu$ should be thought of as describing *incoming* (early time) eigenstates of momentum (particles) in the plane wave limit with physical z -momentum $k^z > 0$ and $-k^z$ for R and L respectively. Modes describing *outgoing* (late time) eigenstates of momenta $\zeta_{\ell,I,k}^\mu$ are instead obtained via

$$\zeta_{\tau_i,\{L,R\}}^\mu = \epsilon_{\tau_i}^\mu \chi_{\tau_i,\{R,L\}}^*(z), \quad (107)$$

$$\zeta_{\lambda,\{L,R\}}^\mu = \left(\frac{-ik^n \partial_z (v \lambda_{\{R,L\}}^*)}{gE v^2}, \frac{E}{g v} \lambda_{\{R,L\}}^* \right) \stackrel{\text{on shell}}{=} \bar{\partial}^\mu \left(\frac{\partial_z (v \lambda_{\{R,L\}}^*)}{E g v^2} \right) + \frac{g v(z)}{E} \lambda_{\{R,L\}}^* \delta_z^\mu, \quad (108)$$

where we have dropped k labels to not clutter the notation. Notice the switch in L, R - labels. Both sets of eigenmodes form a complete orthonormal basis and can

¹⁶See section 2.3 and appendix A.

be used to expand the field operator in eq. (104). The associated Fourier operators carry in and out labels to emphasise that they create/annihilate in and out states in the S -matrix language

$$|k_{\ell,I}^{\text{in}}\rangle \equiv \sqrt{2k_0} (a_{\ell,I,k}^{\text{in}})^\dagger |0\rangle , \quad (109)$$

$$|k_{\ell,I}^{\text{out}}\rangle \equiv \sqrt{2k_0} (a_{\ell,I,k}^{\text{out}})^\dagger |0\rangle , \quad I \in R, L \quad \& \quad \ell \in \tau_1, \tau_2, \lambda . \quad (110)$$

Both satisfy the usual algebra eq. (19) upon quantisation.

Ward identity and current conservation: We now comment on current conservation in the case of spontaneously broken Lorentz symmetry. If the gauge symmetry is preserved, vector bosons can couple only to conserved currents. This is not the case when it is spontaneously broken, but we may still choose to consider coupling to a conserved current¹⁷. In the Lorentz invariant theory, the statement of the current conservation can be expressed in terms of amplitudes. Given an arbitrary process with an external vector leg with momentum k^μ , we have the following identity

$$\mathcal{M}^{(4,J)} \equiv \epsilon_k^\mu \mathcal{M}_\mu^{(4,J)} = (\epsilon_k^\mu + k^\mu) \mathcal{M}_\mu^{(4,J)} , \quad (\text{no wall}). \quad (111)$$

where the $(4, J)$ label indicates full 4-momentum conservation and the process is mediated by the conserved current J^μ , and ϵ_k^μ is the external particle's polarisation vector. This Ward identity implies that substituting the latter for the particle's momentum k^μ makes the amplitude vanish.

In the presence of a domain wall in the z direction, the generalised matrix element $\mathcal{M}^{(3)}$ as defined in eq. (26) includes an integral over z and the polarisation tensor is also a function thereof. The expression of conservation closest to eq. (111) is

$$\mathcal{M}^{(3,J)} \equiv \int dz \chi_{\ell,I,k}^\mu(z) \mathcal{M}_\mu^{(3,J)}(z) = \int dz (\chi_{\ell,I,k}^\mu(z) + \bar{\partial}^\mu f(z)) \mathcal{M}_\mu^{(3,J)}(z) , \quad (112)$$

where $\bar{\partial}^\mu \equiv (-ik^n, \partial^z)$, (with wall)

and $f(z)$ is an arbitrary function.

To make this discussion more concrete we consider the coupling of the gauge field to the conserved current made out of ψ fields we introduced in eq. (56):

$$\mathcal{L} = ig A_\mu J^\mu , \quad J^\mu = i (\psi^\dagger \partial^\mu \psi - \psi \partial^\mu \psi^\dagger) , \quad \partial^\mu J_\mu = 0 . \quad (113)$$

Then the amplitude (defined in eq. (26)) corresponding to the emission of the (l, I) polarisation from the current will be equal to

$$\langle k_I^{\text{out}} q | \mathcal{S} | p \rangle \equiv (2\pi)^3 \delta^{(3)}(p^n - k^n - q^n) \int dz (\zeta_{l,I,k}^\mu(z))^* (p+q)_\mu e^{i(p^z - q^z)z} , \quad (114)$$

where as usual p, q are the initial and final momentum of the ψ particle. Note, modulo a numerical factor, the same expression will be valid for the emission of

¹⁷For example this is the case for the coupling of W boson to light quarks, in the high energy regime when the quark masses can be approximately neglected.

the vector boson from an arbitrary conserved current (not necessarily one made from scalars). The current conservation imposes that any interaction which can be written in the form

$$J^\mu \partial_\mu f \quad \Rightarrow \quad \langle final | \mathcal{S}_f | initial \rangle = \int d^4x \quad \partial_\mu f(x) J^\mu(x) = 0 , \quad (115)$$

has a vanishing matrix element. We see now the use of writing the polarisation vector for the λ d.o.f. as we did in eq. (108). The dangerous-looking first term is actually a total derivative and can be subtracted when computing amplitudes (see appendix B). We comment further on this in the next section as well as discuss the case of non-conserved current in appendix C.

3.5 Subtleties with WKB regime

Before we start computing the amplitudes of interest, we highlight some important subtleties related to the calculation in the WKB regime. As we have discussed in section 2.6, our formulas are valid only if the contribution inside the wall can be ignored. Let us check whether this is a reasonable approximation for the vector emission. Consider the λ and τ cases separately:

- **τ polarisation**

For the τ polarisations we can estimate the contribution to the amplitude inside and outside of the wall and we find:

$$\frac{\mathcal{M}_{\text{inside}}^\tau}{\mathcal{M}_{\text{outside}}^\tau} \simeq \Delta p_z L_w . \quad (116)$$

Similarly to the scalar case discussed in the section 2.6, the contribution inside the wall can be safely ignored.

- **λ polarisation**

Now let us look at the λ polarisation, and the interactions between the current and λ field. Using the expansion for χ_λ^μ field (see for example eq. (89)) we get:

$$\begin{aligned} g J^\mu A^{\mu(\lambda)} &= g(J_n \partial_n \alpha - J_z \chi_z^\lambda) \\ &= J_n \left[\frac{-i k_n}{E v(z)^2} \partial_z (v(z) \lambda(z)) \right] - J_z \frac{E}{v(z)} \lambda(z) , \end{aligned} \quad (117)$$

outside of the wall, when $\lambda = e^{ikx}$ this becomes

$$J_n \left[\frac{k_n k^z}{E v(z)} \right] - J_z \frac{E}{v(z)} \lambda = g J^\mu \cdot \epsilon_\mu^{(\lambda)} , \quad (118)$$

see eq. (86). Let us consider the domain wall connecting the vacua with broken and restored gauge symmetry. In this case, the λ polarisation will interact with

the ψ particle only on the broken side. Then the amplitude originating from the integration outside of the wall will be equal to

$$\mathcal{M}_\lambda^{\text{wkb red.}} \propto - \left(\frac{(p+q)^\mu \epsilon_\mu^{(\lambda)}(z \rightarrow -\infty)}{p^z - q^z - \tilde{k}^z} \right) \simeq - \left(\frac{\tilde{k}^z (p^z + q^z)}{\tilde{v} E} \right),$$

$$\tilde{v} \equiv v(z \rightarrow +\infty), \quad (119)$$

where we have kept only the leading term in energy in the polarisation vector and simplified using the conservation of the current, $p^2 = q^2$. We can see that this matrix element is growing with energy and is singular in the limit $\tilde{v} \rightarrow 0$, which are very worrisome properties since the limit $\tilde{v} \rightarrow 0$ corresponds to the no domain wall and therefore no transition radiation, i.e. $\mathcal{M} \rightarrow 0!$ Let us look now at the contribution coming from the integration inside the wall, using the interaction form of eq. (117)

$$\mathcal{M}_{\text{inside}} \simeq \int_0^{L_w} dz e^{-i(p-q)^z z} (p+q)_n \left[\frac{-ik_n}{E v(z)^2} (\partial_z v(z) + v(z) \partial_z) \right] e^{-i \int_0^z d\bar{z} k^z(\bar{z})}$$

$$- \int_0^{L_w} dz e^{-i(p-q)^z z} (p+q)_z \frac{E}{v(z)} e^{-i \int_0^z d\bar{z} k^z(\bar{z})}. \quad (120)$$

In the first integral there is a term $\propto \partial_z v(z)$, which upon integration will necessarily lead to

$$\mathcal{M}_{\text{inside}} \sim \frac{(p+q)_0}{E} \frac{1}{\tilde{v}}, \quad (121)$$

which is of the same size as the contribution outside of the wall. We see that the amplitude $\mathcal{M}_\lambda^{\text{wkb red.}}$ will definitely lead to incorrect results, so how can we proceed? One possibility would be to take some ansatz for the domain wall and then perform full WKB calculation keeping the terms inside the wall, which will lead to correct results without bad properties of eqs. (120)–(119). However, we can still make progress even without the knowledge of the shape of the wall using the following trick. By construction, we have been focusing on the case where the current built out of ψ fields is conserved

$$J_\mu = i(\psi^\dagger \partial_\mu \psi - \psi \partial_\mu \psi^\dagger), \quad \partial_\mu J^\mu = 0. \quad (122)$$

On the other hand, the λ mode can be written as a complete derivative plus a term subleading in energy (eq. (85))

$$A_\mu^{(\lambda)} = \partial_\mu \alpha + \frac{g v(z)}{E} \lambda(z) (0, 0, 0, 1). \quad (123)$$

The part $\partial_\mu \alpha$ does not couple to a conserved current, meaning that

$$g J^\mu A_\mu^{(\lambda)} \rightarrow - \frac{g^2 v(z)}{E} J_z \lambda. \quad (124)$$

With this simplification, we immediately see that all of the problems with λ polarisations are cured

$$\begin{aligned}\mathcal{M}_{\text{outside}} &\sim \frac{(p+q)^z g^2 \tilde{v}}{E \Delta p_z}, & \mathcal{M}_{\text{inside}} &\sim L_w g^2 \tilde{v} \frac{(p+q)^z}{E}, \\ \frac{\mathcal{M}_{\text{inside}}}{\mathcal{M}_{\text{outside}}} &\sim L_w \Delta p_z.\end{aligned}\tag{125}$$

The contribution inside the wall is suppressed and the matrix element is not growing with energy but vanishes in the limit $\tilde{v} \rightarrow 0$.

So far we have been focusing only on the case when the current made out of ψ fields is conserved on both sides of the wall. This is not true generically, and in particular for SM fermions, where the Yukawa interactions will lead to current non-conservation. So how should one proceed in that case? As explained in more detail in appendix C, it turns out that, with very minor modifications, a very similar trick can be used.

4 Transition radiation and pressure from vectors

We are now ready to calculate transition radiation and the resultant pressure from vector boson emission. We are working in the Abelian Higgs theory of eq. (56) and calculate the average momentum transfer during the radiation of a gauge boson from an incoming ψ particle of energy p^0 . We evaluate the amplitudes of interest in the next section, comment on the final state phase space and masses employed in section 4.2, and finally present our results in section 4.3.

4.1 Amplitudes

All the relevant amplitudes for the particle process $\psi \rightarrow \psi A$ obtained from eq. (114) are reported here. These are τ and λ polarisation emission for left and right movers in the step wall and WKB regimes,

$$\mathcal{M}_{\tau,L}^{\text{step}} = -i g \epsilon_{\tau_2}^\mu (p+q)_\mu \left(\frac{1}{\Delta p_r} + \frac{r_k^\tau}{\Delta p} + \frac{t_k^\tau}{-\Delta \tilde{p}_r} \right),\tag{126}$$

$$\mathcal{M}_{\tau,R}^{\text{step}} = -i g \epsilon_{\tau_2}^\mu (p+q)_\mu \sqrt{\frac{k^z}{\tilde{k}^z}} \left[\frac{\tilde{k}^z}{k^z} \frac{t_k^\tau}{\Delta p} - \frac{1}{\Delta \tilde{p}} + \frac{r_k^\tau}{\Delta \tilde{p}_r} \right],\tag{127}$$

$$\mathcal{M}_\tau^{\text{wkb red.}} = -i g \epsilon_{\tau_2}^\mu (p+q)_\mu \left(\frac{1}{\Delta p} - \frac{1}{\Delta \tilde{p}} \right),\tag{128}$$

$$\mathcal{M}_{\lambda,L}^{\text{step}} = -i \frac{g}{E} (p^z + q^z) \left[g v \left(\frac{1}{\Delta p_r} + \frac{r_k^\lambda}{\Delta p} \right) - g \tilde{v} \frac{t_k^\lambda}{\Delta \tilde{p}_r} \right],\tag{129}$$

$$\mathcal{M}_{\lambda,R}^{\text{step}} = -i \frac{g}{E} (p^z + q^z) \sqrt{\frac{k^z}{\tilde{k}^z}} \left[g v \frac{\tilde{k}^z}{k^z} \frac{t_k^\lambda}{\Delta p} - g \tilde{v} \left(\frac{1}{\Delta \tilde{p}} - \frac{r_k^\lambda}{\Delta \tilde{p}_r} \right) \right],\tag{130}$$

$$\mathcal{M}_\lambda^{\text{wkb red.}} = -i \frac{g}{E} (p^z + q^z) \left[\frac{g v}{\Delta p} - \frac{g \tilde{v}}{\Delta \tilde{p}} \right],\tag{131}$$

where the scattering coefficients $r_k^{\tau,\lambda}$, $t_k^{\tau,\lambda}$ relevant for the amplitudes in the step wall regime are defined in sections 3.3.1 and 3.3.2 and the Δp factors in denominator are defined in eq. (4). We presented amplitudes for $v \neq 0$. However, the symmetry-breaking transition case can be obtained smoothly at this level by sending $v \rightarrow 0$. Note that

$$\mathcal{M}_{\lambda,L}^{\text{step}} \rightarrow 0 \quad \text{as} \quad v \rightarrow 0, \quad (132)$$

in this limit. The discontinuity in asymptotic d.o.f. (and therefore masses) is hidden here inside the kinematic factors and are addressed in the following section.

For λ emission we used current conservation to simplify the computation of these amplitudes by subtracting the total derivative piece in the wavemode eq. (108), as explained in section 2.2. For $\mathcal{M}^{\text{step}}$ this simplification does not change the final expression since it is exact (in the limit of a step wall). However, we emphasise again that it does for $\mathcal{M}_{\lambda}^{\text{wkb red.}}$, which is an approximation as described in section 2.6, and the subtraction is *necessary* to be consistent with the approximations and avoid unphysical divergences, as explained in section 3.5.

4.2 Phase space integration for vector emission

In going from the amplitudes above to the averaged exchanged momentum $\langle \Delta p^\ell \rangle$, where $\ell = \tau, \lambda$, we integrate over final state phase space following the prescriptions and kinematics summarised in section 2.7, using $\mathcal{M}^{\text{step}}$ and $\mathcal{M}^{\text{wkb red.}}$ in their respective regimes of validity. However, there are some important subtleties to discuss compared to the simple theory of scalars of section 2, particularly for a symmetric to broken transition. In this case, the mass of the vector (and therefore τ d.o.f.) in the old phase ($z \rightarrow -\infty$) is zero by gauge invariance since $v = 0$. As shown explicitly in appendix E.4, in principle we can get finite results working with $m = 0$ and integrating over the full phase space as long as the mass of the emitter is kept finite $m_\psi \neq 0$. However, thermal corrections ought to be important. We should expect our calculation to break down for momenta that are too soft (to be defined precisely), where thermal field theory becomes important. To regularise the log divergence in transverse emission when m_ψ is set to zero, [66] cut the k_\perp integration at the soft thermal scale $\sim gT$. This is roughly equivalent to using ‘electric’ thermal masses¹⁸ in all asymptotic state kinematics

$$\begin{aligned} (\tau) : & \begin{cases} \tilde{m} = m_\tau(z = +\infty) \approx g\sqrt{\tilde{v}^2 + T^2}, \\ m = m_\tau(z = -\infty) \approx gT, \end{cases} \\ (\lambda) : & \begin{cases} \tilde{m} = m_\lambda(z = +\infty) \approx g\sqrt{\tilde{v}^2 + T^2}, \\ m = m_\lambda(z = -\infty) = m_{h,s}(T). \end{cases} \end{aligned} \quad \text{(symmetric to broken)} \quad (133)$$

In this work we also impose the IR cut-off in this way, since our primary focus is the proper calculation of λ emission, which turns out to not need IR regulation. We note however that eq. (133) requires further scrutiny. As is well known, the self

¹⁸This is the thermal mass correction in the self-energy of A^0 . It is the relevant scale for example in the Debye screening of the Coulomb field [74].

energy for \vec{A} receives ‘magnetic mass’ thermal corrections only at two loops from charged matter, of parametric order $\sim g^2 T$. Moreover, we are working in the frame of the wall, so the background plasma is boosted and standard results should be distorted. We leave the rigorous inclusion of finite temperature to a follow up study.

In eq. (133), $m_{h,s}$ is the mass of the Higgs d.o.f. in the symmetric phase (see eq. (84)) which will also be temperature dependent¹⁹. So now, for example, the integration limits for the k^z integral for $\langle \Delta p_R^{\lambda, \text{step}} \rangle$ in eq. (46) become explicitly $k^z \in \left[\sqrt{g^2 \tilde{v}^2 + g^2 T^2 - m_{h,s}^2(T)}, k_{\text{max}}^z \right]$ ²⁰.

It is worth stressing that for τ polarisation what appears in the amplitude and in the kinematics boundaries of the PS are always the masses m and \tilde{m} as defined in eq. (133). However, for the λ polarisation the coupling appearing in the amplitude is really the bare $gv(\rightarrow 0)$ and does not receive thermal corrections, while in the kinematics and PS integration what appears is m and \tilde{m} as defined as in eq. (133). So eq. (132) still holds even at finite T . For broken to broken transitions the vector masses are, for both λ and τ fields

$$m \approx g\sqrt{v^2 + T^2}, \quad \tilde{m} \approx g\sqrt{\tilde{v}^2 + T^2}, \quad (\text{broken to broken}). \quad (134)$$

In summary, $\langle \Delta p \rangle$ is computed as in section 2.7 with phase space integration limits in Table 1 and asymptotic masses defined here above. In general, there is a total of six contributions:

$$\begin{aligned} & \langle \Delta p_R^{\tau, \text{step}} \rangle, & \langle \Delta p_R^{\tau, \text{wkb}} \rangle, & \langle \Delta p_L^{\tau, \text{step}} \rangle, \\ & \langle \Delta p_R^{\lambda, \text{step}} \rangle, & \langle \Delta p_R^{\lambda, \text{wkb}} \rangle, & \langle \Delta p_L^{\lambda, \text{step}} \rangle. \end{aligned} \quad (135)$$

4.3 Pressure on the bubble wall

We now report and comment on our results for the average NLO momentum transfer $\langle \Delta p \rangle$ due to transition radiation from a ψ particle travelling across the wall and thereby compute the total pressure on the bubble wall. We show a break down of figs. 2 and 3 into all their contributions, as well as provide some analytical formulae. A comprehensive comparison (via numerical integration - see appendix E for some analytical evaluation of phase space integrals) of all the different parts in eq. (135) is shown in figs. 7 and 8, as a function of the energy of the incoming emitter particle, ψ . In the asymptotic $p_0 \rightarrow \infty$ limit all contributions are constant. Their relative importance is displayed in fig. 9. We now discuss the two cases of interest $v = 0$ and $v \neq 0$ separately.

Symmetric to broken case ($v = 0$). We observe in fig. 7 that when the emitting particle is $m_\psi \lesssim m$ the contribution from τ saturates quickly to the constant $p_0 \rightarrow \infty$

¹⁹We do not discuss the explicit form of it since our results are largely insensitive to it.

²⁰When $m_{h,s}(T) < \tilde{m}(T)$ we are in line with our set up which assumed $m < \tilde{m}$, but if it is the other way around the lower limit of k^z becomes imaginary. This is signaling the fact that modes with $0 < \tilde{k} < \sqrt{m^2 - \tilde{m}^2}$ are now exponentially decaying in the old phase (right) side of the wall. Then it is more appropriate to define the step wall regime according to $k < \tilde{k} \lesssim L_w^{-1}$ and parameterise the PS integrals in terms of (\tilde{k}^z, k_\perp^2) . The integration limits for \tilde{k}^z for R -mover emission would be $\tilde{k}^z \in [0, \tilde{k}_{\text{max}}^z]$, where $\tilde{k}_{\text{max}}^z = \sqrt{(p_0 - m_\psi)^2 - \tilde{m}^2}$.

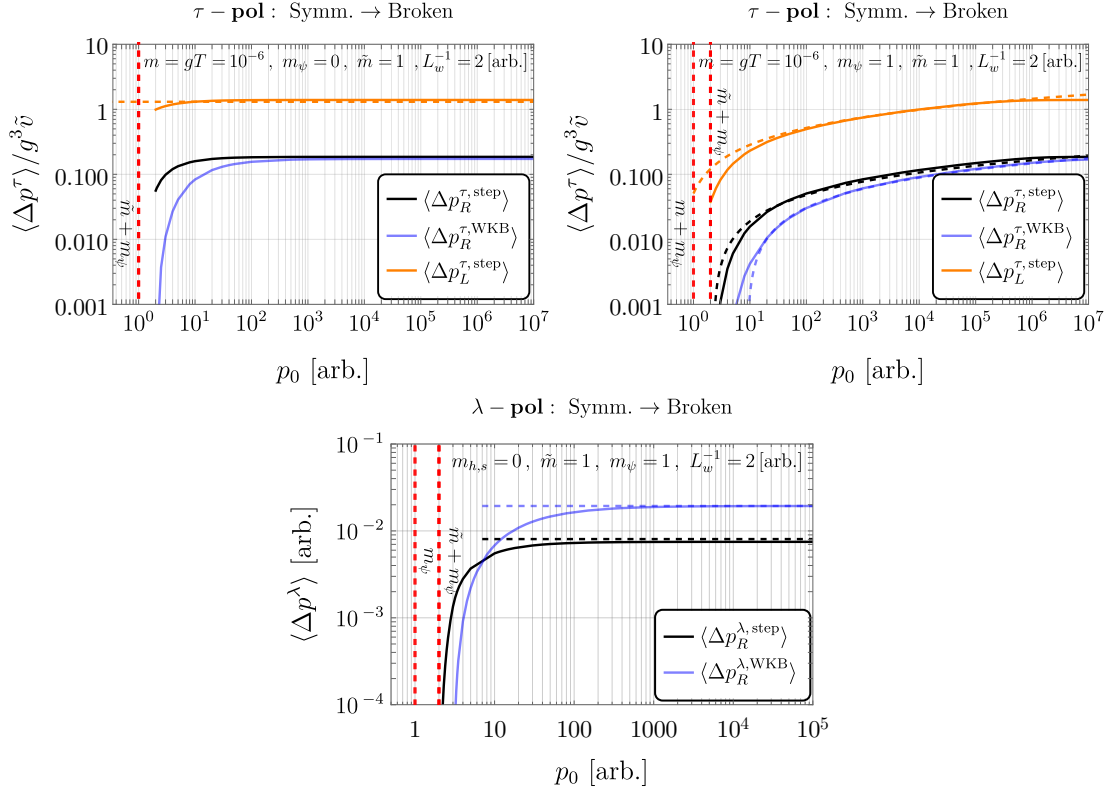


Figure 7: Symmetric \rightarrow Broken. We present qualitatively the same plot as in fig. 3 (left panel), this time disentangling all the contributions, and highlighting the effect of a hierarchy $m \ll m_\psi$ for τ emission. **Top Left:** Averaged momentum exchange for τ polarisation contributions. The curves quickly saturate to their constant asymptotic values and the dominant contribution is L -mover emission in the step wall regime. Thick lines are numerics and the dashed line is the analytical expression in eq. (201). **Top Right:** Same as previous, but for $m/m_\psi \ll 1$. We see the transient inter-relativistic regime scaling as $\log(p_0)$, well described by the $m = 0$ analytical formulae (dashed lines) found in appendix E.4. The regime ends around $p^0 \sim \tilde{m}m_\psi/m$. **Bottom:** λ polarisation contributions. The result is quite insensitive to the symmetric side λ mass $m_{h,s}(T)$ as long as it is $\lesssim \tilde{m}$. We plot for $m_\psi = 1$ [arb.], but varying it does not change much either; unlike for τ , there is no intermediate regime. Dashed lines are analytical formulae in eqs. (209) and (210).

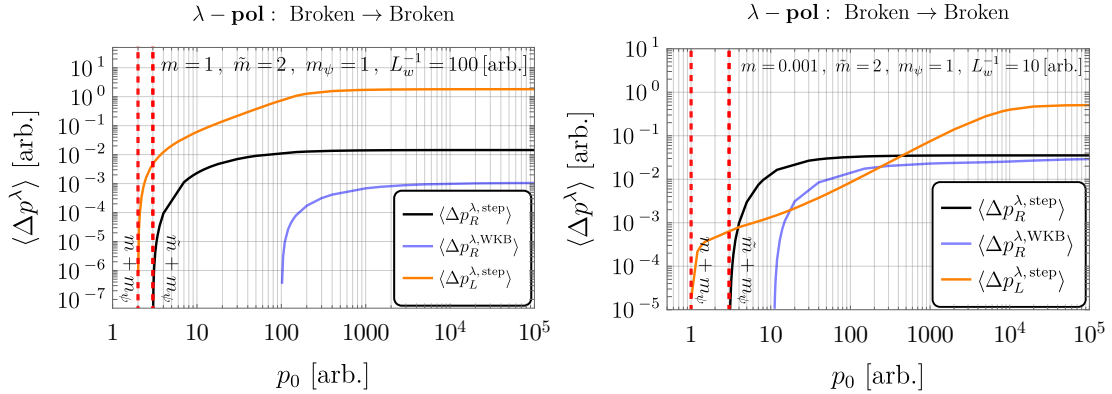


Figure 8: Broken \rightarrow Broken. **Left:** Averaged momentum exchange for λ polarisation emission for relatively thin wall. The inter-relativistic regime of scaling with p^0 lasts till $p^0 \sim L_w^{-1}$. Taking $\Delta m \ll 1$ does not qualitatively change anything except for suppressing all values. Notice $m \lesssim \tilde{m}$. **Right:** Similar to previous, but in the case $m \ll \tilde{m}$. Here we see that the inter-relativistic regime is distorted at low p^0 and also extended up to $p_0 \sim L_w^{-1} m_\psi / m$.

value (top left in fig. 7), but if there is a hierarchy $m \ll m_\psi$, we observe an inter-relativistic regime of logarithmic dependence on p_0 up until $p_0 \sim \tilde{m} m_\psi / m$. This can be traced to a collinear log divergence of phase space integration in the limit $m = 0$ & $p_0 \rightarrow \infty$ as explained in appendix E. This behaviour is not present in contributions from λ polarisation emission, which are insensitive to m_ψ for relativistic p^0 , even when the symmetric side mass is set to zero $m_{h,s} = 0$.

In the asymptotic $p^0 \rightarrow \infty$ limit τ contributions depend significantly only on the ratio²¹ m/\tilde{m} , which can be translated to T/\tilde{v} . While individual λ contributions depend also on L_w^{-1} their sum is constant. The total momentum transfer (summing over all contributions) can be fitted by the following expression

$$\lim_{p_0 \rightarrow \infty} \langle \Delta p^{\text{total}} \rangle \simeq g^3 \tilde{v} \left[0.135 \log \left(\frac{\tilde{v}}{T} + 2.26 \right) - 0.085 - 0.2 \frac{\log \left(\frac{\tilde{v}}{T} + 2.26 \right)}{\tilde{v}/T} + \frac{0.19}{\tilde{v}/T} \right]. \quad (136)$$

We recall that to obtain this expression we cut the phase space integrals in the IR at energies $\sim gT$. The expression in eq. (136) becomes valid for the energies of initial particle $p_0 \gtrsim \frac{\tilde{v}}{T} \times m_\psi$, which in the case of massless emitter $m_\psi \rightarrow 0$ becomes $p_0 \gtrsim \tilde{v}$. At last we would like to remind the reader that the expression above was obtained just for the single vector emission, and one cannot trust it for very large values of log.

The contribution of the longitudinal modes is sub-leading except perhaps for mild super-cooling $\tilde{v}/T \sim \text{few}$, and is equal approximately to

$$\lim_{p_0 \rightarrow \infty} \langle \Delta p^\lambda \rangle \sim g^3 \tilde{v} \times c_\lambda(L_w, T, \tilde{m}, m_\psi), \quad c_\lambda \in [0.02, 0.03]. \quad (137)$$

This result qualitatively agrees with the estimate in the Ref. [63]. An analytical form for the function c_λ is given in eq. (211).

²¹See for example the exact evaluation of the dominant contribution eq. (201).

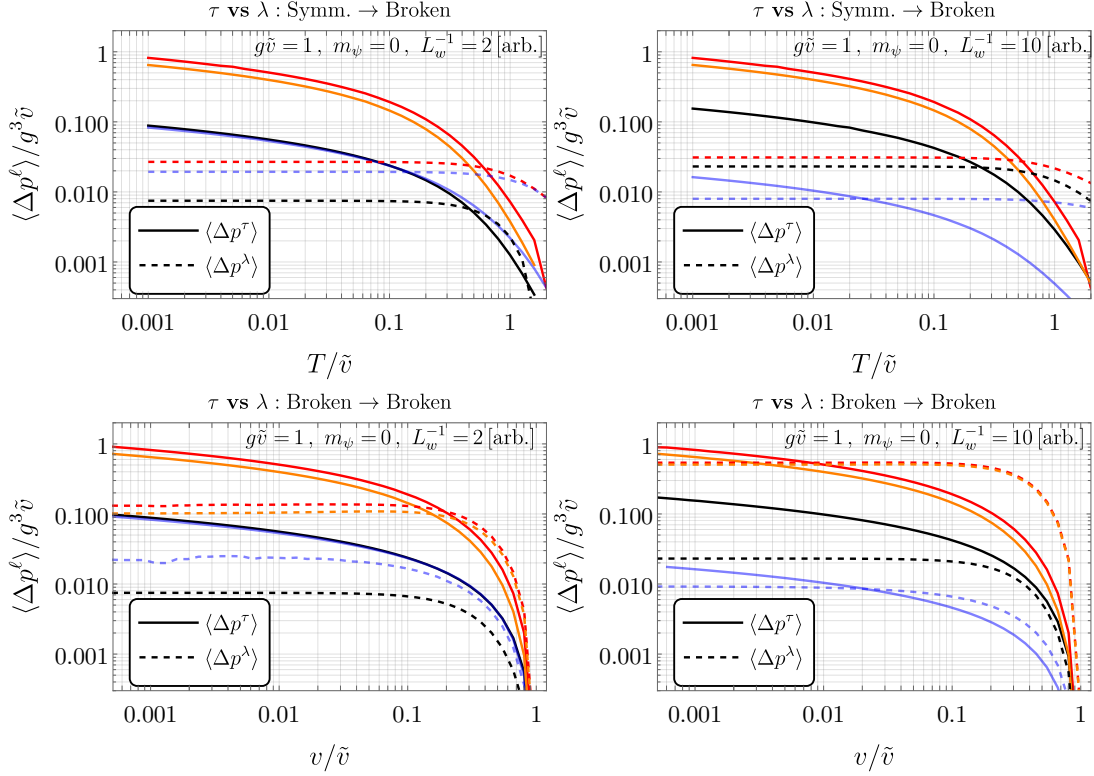


Figure 9: Here is presented the same plot as in fig. 2, but this time disentangling all the contributions. Solid lines refer to τ polarisation, while dashed to λ . The red lines are the total sum, for each polarisation. **Top:** Symmetric \rightarrow Broken. It is shown two cases with different wall widths and it is worth noticing that while the total contribution for τ and λ does not change appreciably, the single contributions do, like R step wall versus WKB. **Bottom:** Broken \rightarrow Broken. Here it happens the same as in the top panels, but, since in this case, L step contribution from λ polarisation has to be taken into account, we see that, depending on the value of L_w and the hierarchy between the different vevs, can be the most relevant contribution.

So far we have been calculating the momentum transfer from individual collisions. In order to find the pressure acting on the bubble wall we need to perform the integration over the flux of incoming particles. This can be easily done in the thermal case since we know the distributions

$$\mathcal{P} = \int \frac{d^3p}{(2\pi)^3} f_\psi(T, \gamma_w) \times \frac{p^z}{p_0} \langle \Delta p \rangle. \quad (138)$$

If the average momentum transfer is a constant the integration is simple and we find, since in the ultra-relativistic case $p^z/p_0 \rightarrow 1$,

$$\mathcal{P} = n_\psi(T, \gamma_w) \langle \Delta p \rangle = \gamma_w n_\psi(T) \langle \Delta p \rangle, \quad (139)$$

where n_ψ is the density of emitters ψ defined in the plasma frame. Then, for the symmetric to broken transition we obtain the following expression for the pressure:

$$\lim_{\gamma_w \rightarrow \infty} \mathcal{P}_{\text{th.}} \simeq \frac{\zeta(3) \gamma_w T^3}{\pi^2} \times \quad (140)$$

$$g^3 \tilde{v} \left[0.135 \log \left(\frac{\tilde{v}}{T} + 2.26 \right) - 0.085 - 0.2 \frac{\log \left(\frac{\tilde{v}}{T} + 2.26 \right)}{\tilde{v}/T} + \frac{0.19}{\tilde{v}/T} \right],$$

where th. stands for thermal.

Broken to broken case ($v \neq 0$). In fig. 8 we show the evolution of $\langle \Delta p \rangle(p_0)$ for a broken to broken transition. We focus only on λ contributions since the ones from τ are essentially the same as in fig. 7 with suitable re-interpretation of what m, \tilde{m} mean (see section 4.2). Again the curves eventually saturate to a constant value but we highlight the strongly L_w -dependent novel contribution from L -mover emission, which easily comes to dominate in the thin wall regime. As in fig. 3, we highlight that in the left panel, we can clearly distinguish the inter-relativistic region where this last contribution develops a linear growth in p_0 . In fig. 9 we see the dependence of the saturation value of the averaged exchanged momentum (in the limit $p_0 \rightarrow \infty$) on the ratio between vevs (lower panels).

Broken to broken transitions were recently studied at leading order by [68] and it was found that reflection of the longitudinal vectors is efficient for the energies below L_w^{-1} (inverse width of the wall). This in its turn leads to the pressure scaling as γ_w^2 , as long as $p_0 < L_w^{-1}$. We find that a reminiscent effect happens at NLO level, the main difference is that the momentum of the vector is not fixed by the speed of the bubble expansion and is always integrated over all possible values. We find that the momentum transfer is dominated by left-mover modes and for the values of the energies of incoming particle $p_0 < L_w^{-1} \text{Max}[1, m_\psi/m]$ it is proportional to $\propto p_0$

$$\lim_{p_0 < L_w^{-1} \text{Max}[1, m_\psi/m]} \langle \Delta p_{v \neq 0} \rangle \sim 10^{-2} \times g^2 \frac{(v^2 - \tilde{v}^2)^2}{(v^2 + \tilde{v}^2)^2} \times \frac{p_0}{\text{Max}[1, m_\psi/m]}. \quad (141)$$

In the case of large hierarchy $0 < m \ll m_\psi$, not only is the saturation point delayed, but a further slight distortion occurs at low p^0 , as shown in fig. 8. Once the energy of the initial particle becomes larger than $\sim L_w^{-1} \text{Max}[1, m_\psi/m]$, we have

$$\lim_{p_0 \rightarrow \infty, L_w \rightarrow 0} \langle \Delta p_{v \neq 0} \rangle \simeq 0.05 g^2 \frac{(v^2 - \tilde{v}^2)^2}{(v^2 + \tilde{v}^2)^2} L_w^{-1}. \quad (142)$$

Momentum transfer stops growing and reaches the saturation value. Note that the maximal value of this pressure is controlled by L_w^{-1} and not by the mass of the vector $g\tilde{v}$. This is related to the fact that at high energies Goldstone Boson equivalence theorem relates the longitudinal vectors to the Goldstone bosons, and the strength of their interaction with the bubble wall (Higgs field) is controlled by the mass of the Higgs (wall width). Consequently, in the case of broken to broken transition, there is an additional contribution to the pressure which scales as

$$\lim_{\gamma_w \rightarrow \infty} \mathcal{P}_{v \neq 0}^\lambda \sim 0.05 \frac{\zeta(3) \gamma_w T^3}{\pi^2} \times g^2 \frac{(v^2 - \tilde{v}^2)^2}{(v^2 + \tilde{v}^2)^2} \times L_w^{-1}. \quad (143)$$

with an intermediate regime scaling as $\mathcal{P}^\lambda \propto \gamma_w^2$ for the values of boost factor $\gamma_w < (L_w T)^{-1}$.

5 Summary

We conclude by summarising the main results of our work. We analyzed in detail the phenomena of transition radiation in the presence of domain walls. We quantised from first principles scalar and vector theories on a translation-violating background and identified the correct asymptotic states. We split emission into soft and UV regimes and used a step wall and WKB approximation respectively to compute the desired matrix elements for transition radiation. Quantisation of vector field theories was naturally performed via the introduction of new degrees of freedom which do not coincide with the traditional transverse and longitudinal polarisation but are a convenient admixture. In this way, we have resolved some puzzles regarding the inclusion of longitudinal polarisations in the calculation of transition radiation.

We applied these results to calculate the pressure experienced by the bubble wall during the ultra-relativistic expansion. For the phase transitions with spontaneous breaking of the gauge symmetries in the regime of strong supercooling, we find the pressure which scales as

$$\mathcal{P} \propto \gamma_w g^3 \tilde{v} T^3 \log \frac{\tilde{v}}{T}, \quad \text{for } \tilde{v}/T \gg 1, \quad (144)$$

and is dominated by the emission back out of the wall of transverse-like polarisations with momenta $k^z \in (0, \Delta m)$. This result qualitatively agrees with the previous literature on the subject. For moderate ratio $\tilde{v}/T \sim \text{few}$ we find that the contribution from the longitudinal-like polarisations can lead to significant corrections. We provide an updated fitted formula for the total pressure in eq. (140).

We also analyzed the pressure in the case of transition between two vacua with broken gauge symmetry. Interestingly we find in this case the contribution from the longitudinal-like polarisation can easily become dominant for thin walls, with the asymptotic value controlled by the inverse wall width $\mathcal{P}^{\text{max}} \propto \gamma_w g^2 T^3 L_w^{-1}$. Moreover, we find a transient intermediate regime of $\mathcal{P} \propto \gamma_w^2$ scaling for $p_0 \lesssim L_w^{-1}$.

Our results make an advance in understanding the balance between bubble acceleration and friction which plays a crucial role in determining most phenomenological consequences of FOPTs as well as their detection prospect at upcoming gravitational wave detectors.

Future outlook: The work can be improved and generalised in several ways. An important remaining question is the inclusion of finite temperature effects in a robust first principles fashion (see for example the discussion in section 4.2). It is relatively easy, though cumbersome, to allow also for the emitting particle to feel the wall $m_\psi \rightarrow m_\psi(z)$. Though in the $\gamma_w \rightarrow \infty$ limit, any dependence on $m_\psi(z)$ should drop out, we saw how m_ψ can distort the intermediate shape of $\mathcal{P}^{\text{NLO}}(\gamma_w)$ and ultimately finding the equilibrium velocity v_w will require full knowledge of this curve. Similarly one could rigorously quantise fermionic fields that change mass across the wall.

A possibly important direction is the analysis of multiple vector emissions, particularly in regimes with large logs, possible IR enhancements, and back-reaction effects coming from the overdensity of soft vector bosons around the wall (see discussion in [66]). Furthermore, it would be interesting to compare our wall-shape-independent results with a full numerical calculation using a specific smooth wall ansatz (for example *tanh*). Finally, with some tweaks, our expressions can be used to analyse pressure in qualitatively different types of FOPTs, such as spontaneous breaking of *global* symmetries, or even symmetry *restoring* transitions.

While our interest here was in friction, we emphasise that our set up is useful for rigorously computing any process / Feynman diagram²² in the presence of background walls which are not treated as a perturbation. Just as an example, one can easily re-purpose our expressions to compute the number of particles of a given species produced from collisions between an expanding bubble and surrounding particles²³. The spontaneous breaking of Lorentz/translational symmetry in the early universe results in a rich phenomenology that is only starting to be explored systematically.

Acknowledgements

AA is supported by the MUR contract 2017L5W2PT. MV is supported by the “Excellence of Science - EOS” - be.h project n.30820817, and by the Strategic Research Program High-Energy Physics of the Vrije Universiteit Brussel. AA and GB would like to thank M. Serone for discussions. RPB is very grateful to Giacomo Koszegi for numerous discussions at the preliminary stages of the project and wishes him all the best in his new career. RPB also thanks Giovanni Villadoro and Mehrdad Mirbabayi for illuminating discussions. We thank Anson Hook and Isabel Garcia Garcia for feedback on the draft.

²²At tree or even loop level.

²³These could be heavy, Dark matter candidates.

A Wavepackets and asymptotic states

No wall: Let us recall a few things in the usual manifestly translation-invariant case (no wall background). For clarity, we will first focus on 1 + 1 dimensions. For a scalar field theory, the field operator $\psi(t, z)$ is interpreted as creating a particle at position z at time $t = 0$. The position space wavefunction of a state is thus given by its inner product with $\langle 0|\psi$. The wavefunction of a single particle eigenstate of momentum $|k\rangle = \sqrt{2k^0}a_k^\dagger|0\rangle$ is, as expected,

$$\langle 0|\psi(t, z)|k\rangle = e^{-ik_\mu x^\mu} . \quad (145)$$

To derive formulae for observables such as scattering cross sections or emission probabilities involving realistic particles we have to crucially go through appropriately defined wavepackets that describe those asymptotic states, taking a limit of sharp momentum only at the end. A wavepacket state describing a particle with momentum peaked around p and localised in space is given by

$$|\Psi_p\rangle \equiv \int_{-\infty}^{\infty} \frac{dk^z}{(2\pi)\sqrt{2k^0}} f_p(k^z)|k\rangle , \quad \langle \Psi_p|\Psi_p\rangle = \int \frac{dk^z}{(2\pi)} |f_p(k^z)|^2 = 1 . \quad (146)$$

where $f_p(k^z)$ is like a sharp Gaussian in k^z peaked at p^z . Note there is no spacetime dependence in this expression (we are always in the Heisenberg picture). The limit to recover a momentum eigenmode is $f_p(k^z) \rightarrow (2\pi)^3 \sqrt{2k^0} \delta(p^z - k^z)$. However, the more appropriate limit used in the derivation of physical rates makes use of the normalisation condition above

$$|f_p(k^z)|^2 \rightarrow (2\pi)\delta(p^z - k^z) , \quad (\text{peaked momentum limit}) . \quad (147)$$

To see the localisation we can look at the wavefunction of the wavepacket state:

$$\langle 0|\psi(t, z)|\Psi_p\rangle = \int_{-\infty}^{\infty} \frac{dk^z}{(2\pi)\sqrt{2k^0}} f_p(k^z) e^{-ik_\mu x^\mu} . \quad (148)$$

At $t = 0$ this is an oscillating function of z (with wavelength controlled by p) with a Gaussian envelope so that it is indeed localised at $z = 0$. As a function of time, the wavepacket moves in the direction of $\text{sign}(p)$. Because each mode has a slightly different dispersion relation, the spatial width of the wavepacket tends to widen in time (dispersion) but this can be counteracted by making $f_p(k)$ a sharper Gaussian, taking an appropriate order of limits.

A.1 Asymptotic states in the wall background

In the presence of the wall we should still define asymptotic particle states as appropriate wavepackets to compute formulae for physical rates. A slight complication comes from the fact that the one particle states $|k_{L,R}\rangle$ we quantise are not eigenstates of momentum. Moreover, in general, the same state describes different types of particles in different regions of space²⁴. Defining the asymptotic state carefully will get rid of any ambiguity.

²⁴This can be simply because the mass changes or, as in the case of $\lambda(x)$ in a symmetric to broken transition, the field interpolates even between particles of different spin.

We now consider an operator that feels the wall $\phi(t, \vec{x})$ expanded in left and right mover modes as in eq. (17). As before, the action of this on the vacuum should be thought of as creating a particle localised at $x^\mu = 0$. Contracting a state with $\langle 0|\phi$ still gives the wavefunction understood in the usual sense. In fact

$$\langle 0|\phi(t, \vec{x})|k_I\rangle = e^{-ik_n x^n} \chi_{I,k}(z) , \quad (149)$$

with $I = R, L$. To gain physical intuition of the one particle states $|k_I\rangle$, consider constructing wavepackets by superimposing exclusively right (left) movers:

$$|\Phi_{I,p}^{\text{in}}\rangle \equiv \int_{0, \Delta m}^{\infty} \frac{dk^z}{(2\pi)\sqrt{2k^0}} f_p(k^z) |k_I\rangle , \quad (150)$$

where again we focus on 1 + 1 dimensions and where the lower limit is 0 (Δm) for R (L) movers respectively. The ‘in’ labels will become clear shortly. Their wavefunctions are respectively

$$\langle 0|\phi(t, z)|\Phi_{I,p}^{\text{in}}\rangle \equiv \int_{0, \Delta m}^{\infty} \frac{dk^z}{(2\pi)\sqrt{2k^0}} f_p(k^z) e^{-ik^0 t} \chi_{I,k}(z) . \quad (151)$$

Ignoring the slight dispersion mentioned at the end of the previous subsection, the time evolution of eq. (151) for $I = R(L)$ describes an isolated localised wavepacket travelling in towards the wall from $z < 0$ ($z > 0$) when $t < 0$. This wavemode scatters off the wall and for $t > 0$ splits into reflected and transmitted wavemodes travelling in opposite directions. Thus, $|\phi_{R,p}^{\text{in}}\rangle$ ($|\phi_{L,p}^{\text{in}}\rangle$) is a good asymptotic state for an *incoming* particle with positive (negative) z -momentum. It cannot however be used as an asymptotic state for any single *outgoing* asymptotic particle since at late times it describes a superposition.

So what about single localised *outgoing* particles? Clearly, when the wave equation is reduced to Schrodinger-like form with a real potential, these can be obtained by complex conjugation of the spacial part of the wavefunction. In other words we require states $|\Phi_{I,p}^{\text{out}}\rangle$ such that

$$\langle 0|\phi(t, z)|\Phi_{I,p}^{\text{out}}\rangle \equiv \int_{\Delta m, 0}^{\infty} \frac{dk^z}{(2\pi)\sqrt{2k^0}} f_p(k^z) e^{-ik^0 t} \zeta_{I,k}(z) , \quad (152)$$

$$\text{with } \zeta_{R,L}(z) = \chi_{L,R}^*(z) .$$

In time, these correspond to two waves coming from opposite sides of the wall, hitting the wall around $t \approx 0$ and interfering in just the right way so that at late time there is only one wavemode travelling towards $z \rightarrow -\infty$ or $z \rightarrow \infty$ respectively. Notice the swap in labels. We adopt the convention that the right-mover R (left-mover L) label always denotes a particle of positive (negative) z -momentum. It is an easy exercise to write the $\zeta_{R,L}$ in terms of a linear composition of the complete basis $\chi_{R,L}$ as explicitly done in eqs. (22) and (23). The appropriate wavepacket for an outgoing state is thus

$$|\Phi_{I,p}^{\text{out}}\rangle \equiv \int_{\Delta m, 0}^{\infty} \frac{dk^z}{(2\pi)\sqrt{2k^0}} f_p(k^z) |k_I^{\text{out}}\rangle , \quad (153)$$

where $|k_I^{\text{out}}\rangle$ are the one-particle states with wavefunctions $\zeta_{I,k}(z)$ and are related to the $|k_I\rangle$ by

$$|k_L^{\text{out}}\rangle = r_{R,k}^* |k_R\rangle + t_{R,k}^* \sqrt{\tilde{k}^z/k^z} |k_L\rangle \Theta(k^z - \Delta m), \quad (154)$$

$$|k_R^{\text{out}}\rangle = t_{L,k}^* \sqrt{k^z/\tilde{k}^z} |k_R\rangle + r_{L,k}^* |k_L\rangle, \quad (155)$$

where the reflection and transmission coefficients were defined in general for scalar d.o.f. in section 2.1, and given explicit form in the case of a step wall for fundamental scalars also in section 2.1 and for different vector polarisations in section 3.3.

Reflection and transmission probabilities: As a consistency check, we can compute reflection and transmission probabilities in this language. Focusing on the identity part of the S matrix $S = 1 + i\mathcal{A}$, the amplitude for a particle incoming from $z < 0$ to reflect and transmit should be, respectively:

$$\langle \phi_{L,p}^{\text{out}} | \phi_{R,p}^{\text{in}} \rangle = \int_0^\infty \frac{dk}{2\pi} |f_p(k)|^2 r_{R,k} \rightarrow r_{R,p}, \quad (156)$$

$$\langle \phi_{R,p}^{\text{out}} | \phi_{R,p}^{\text{in}} \rangle = \int_{\Delta m}^\infty \frac{dk}{2\pi} |f_p(k)|^2 t_{L,k} \sqrt{\tilde{k}^z/k^z} \rightarrow \begin{cases} t_{L,p} \sqrt{p/\tilde{p}}, & p > \Delta m \\ 0, & p < \Delta m \end{cases}, \quad (157)$$

where the arrow denotes taking the peaked momentum limit eq. (147) in the end. So the relative probability for a peaked-around- p incoming mode to reflect/transmit into a peaked-around- p outgoing mode is what one could have already guessed

$$\text{Reflection probability} = |\langle \phi_{L,p}^{\text{out}} | \phi_{R,p}^{\text{in}} \rangle|^2 \rightarrow |r_{R,p}|^2, \quad (158)$$

$$\text{Transmission probability} = |\langle \phi_{R,p}^{\text{out}} | \phi_{R,p}^{\text{in}} \rangle|^2 \rightarrow \begin{cases} |t_{L,p}|^2 p/\tilde{p}, & p > \Delta m \\ 0, & p < \Delta m \end{cases}. \quad (159)$$

A.2 Phase space derivation from wavepackets

In this section we will obtain formulae for the averaged momentum exchanged by transition radiation processes in the background of the wall, deriving eq. (33) in the main text. Treating the incoming particle as a wavepacket as in eq. (146), we find the amplitude squared for splitting into ℓ particles, which may or may not feel the wall. These outgoing states are late-time eigenstates of momentum, obtained as limits of their own wave-packet forms. We have

$$\begin{aligned} |\langle k_1^{\text{out}} \dots k_\ell^{\text{out}} | \Phi_p \rangle|^2 &= \int \frac{d^3 p_1 d^3 p_2}{\sqrt{4p_1^0 p_2^0}} f_p(p_1) f_p^*(p_2) \delta^{(3)}\left(p_1 - \sum_{i=1}^{\ell} k_i\right) \delta^{(3)}\left(p_2 - \sum_{j=1}^{\ell} k_j\right) |\mathcal{M}_{1 \rightarrow \ell}^{(3)}|^2 \\ &= \int \frac{d^3 p_1 d p_2^z}{\sqrt{4p_1^0 p_2^0}} f_p(p_1) f_p^*(p_2) \delta^{(3)}\left(p_1 - \sum_{i=1}^{\ell} k_i\right) \frac{p_1^0}{|p_1^z|} \delta(p_1^z - p_2^z) |\mathcal{M}_{1 \rightarrow \ell}^{(3)}|^2 \\ &= \int \frac{d^3 p_1}{2|p_1^z|} |f_p(p_1)|^2 \delta^{(3)}\left(p_1 - \sum_{i=1}^{\ell} k_i\right) |\mathcal{M}_{1 \rightarrow \ell}^{(3)}|^2 \\ &\rightarrow \frac{(2\pi)^3}{2|p^z|} \delta^{(3)}\left(p - \sum_{i=1}^{\ell} k_i\right) |\mathcal{M}_{1 \rightarrow \ell}^{(3)}|^2, \end{aligned} \quad (160)$$

where the temporary label (3) on \mathcal{M} emphasises only three of 4-momentum are conserved. In the last step, we take the peaked momentum limit of eq. (147). For the particular case of a $1 \rightarrow 2$ process as discussed in this work, we have

$$\begin{aligned}
\langle \Delta p_{I=R,L}^z \rangle &\equiv \int \mathcal{P}_{p \rightarrow q k_I^{\text{out}}} \Delta p_I^z = \int \frac{d^3 k}{(2\pi)^3 2k^0} \int \frac{d^3 q}{(2\pi)^3 2q^0} |\langle q k_I^{\text{out}} | \Phi_p \rangle|^2 \Delta p_I^z \\
&= \int \frac{d^3 k d^3 q}{(2\pi)^3 8p^z k^0 q^0} \delta^{(3)}(p - k - q) |\mathcal{M}_I^{(3)}|^2 \Delta p_I^z \\
&= \int \frac{d^3 k}{(2\pi)^3 8p^z k^0 |q_k^z|} \left[|\mathcal{M}_I^{(3)}|^2 \Delta p_I^z \right]_{q^z = \pm q_k^z} \quad (161)
\end{aligned}$$

where in going to the last line we have used

$$\begin{aligned}
\delta(p^0 - k^0 - q^0) &= \frac{q^0}{|q_k^z|} [\delta(q^z - q_k^z) + \delta(q^z + q_k^z)] \\
\text{with } q_k^z &= \sqrt{(p^0 - k^0)^2 - k_\perp^2 - m_q^2} \quad (162)
\end{aligned}$$

Thus, in principle, one should sum contributions from both signs of q^z to obtain the full integrated rate. In practice, the $q^z < 0$ branch will be highly sub-leading at large energies.

Comparison with decay formula: One might wonder how to recover the familiar decay formula in the limit of no wall. The latter can be derived in terms of the full 4-momentum conserving matrix element $\mathcal{M}^{(4)}$ as

$$\begin{aligned}
|\langle k_1 \dots k_\ell | p \rangle|^2 &= \int \frac{d^3 p_1 d^3 p_2 (2\pi)^2}{\sqrt{4p_1^0 p_2^0}} f_p(p_1) f_p^*(p_2) \delta^{(4)}\left(p_1 - \sum_{i=1}^{\ell} k_i\right) \delta^{(4)}(p_2 - p_2) |\mathcal{M}_{1 \rightarrow \ell}^{(4)}|^2 \\
&= \int \frac{d^3 p_1 (2\pi)^2}{2p_1^0} |f_p(p_1)|^2 \delta^{(4)}\left(p_1 - \sum_{i=1}^{\ell} k_i\right) \underbrace{\delta(0)}_{T/2\pi} |\mathcal{M}_{1 \rightarrow \ell}^{(4)}|^2 \\
&\longrightarrow \frac{(2\pi)^4}{2p_0} \mathbb{T} \delta^{(4)}\left(p - \sum_{i=1}^{\ell} k_i\right) |\mathcal{M}_{1 \rightarrow \ell}^{(4)}|^2, \quad (163)
\end{aligned}$$

where \mathbb{T} is total time (one can only define a decay probability per unit time). We can see how eq. (160) reduces to this result. In the absence of the wall, the matrix element gives

$$|\mathcal{M}_{1 \rightarrow \ell}^{(3)}|^2 = 2\pi \mathbb{L}^z \delta\left(p^z - \sum_{i=1}^{\ell} k_i^z\right) |\mathcal{M}_{1 \rightarrow \ell}^{(4)}|^2 \quad (164)$$

where \mathbb{L}^z is the distance traversed in the z direction. Finally, using that $\mathbb{L}^z = \mathbb{T} p^z/p^0$, eq. (160) reduces to eq. (163).

B Current conservation in the presence of the wall

In the main text, we have discussed the modifications of the Ward identities in the presence of the wall and that in general the conserved current coupled to the total

derivative must give zero matrix element,

$$J^\mu \partial_\mu f \quad \Rightarrow \quad \langle final | \mathcal{S}_f | initial \rangle = 0 . \quad (165)$$

Let us discuss the effects of various choices of the gauge transformation function f . For example let us consider $f = \chi_{1,2}^\tau(z)$, where $\chi_{1,2}^\tau$ are the wave functions for the τ polarisations (see section 3.2). Then the matrix element will be equal to

$$J^\mu \propto (p+q)^\mu \quad \Rightarrow \quad \mathcal{M} = \frac{(p+q)_\mu k^\mu}{\Delta p} + r_k^\tau \frac{(p+q)_\mu k_r^\mu}{\Delta p_r} - t_k^\tau \frac{(p+q)_\mu \tilde{k}^\mu}{\Delta \tilde{p}} ,$$

$$k_r^\mu \equiv (k^m, -k^z), \quad \tilde{k}^\mu \equiv (k^m, \tilde{k}^z) . \quad (166)$$

We can simplify the amplitude using the following identities:

$$(p+q)_\mu k^\mu = (p+q)_m k^m - (p+q)_z k^z$$

$$\stackrel{k_m = (p-q)_m}{=} (p+q)_m (p-k)^m - (p+q)_z k^z$$

$$= p_z^2 + m_\psi^2 - q_z^2 - \tilde{m}_\psi^2 - (p+q)_z k^z$$

$$\stackrel{m_\psi^2 = \tilde{m}_\psi^2}{=} (p+q)_z (p-q-k)^z = (p+q)_z \Delta p . \quad (167)$$

Performing similar manipulations for all of the terms we get:

$$\mathcal{M} = (p+q)_z (1 + r_k^\tau - t_k^\tau) = 0 , \quad (168)$$

where we used the fact that $1 + r_k^\tau - t_k^\tau = 0$ for τ polarisations, as expected. Similarly we can choose $f = \alpha(z)$, of the λ . Then from the eq. (100) we can get

$$\alpha|_{z<0} = \frac{ik^z}{gvE} (e^{ik^z z} - r_k^\lambda e^{-ik^z z}) ,$$

$$\alpha|_{z>0} = it_k^\lambda \times \frac{\tilde{k}^z}{gE\tilde{v}} e^{i\tilde{k}^z z} , \quad (169)$$

where we have used that $\alpha = \frac{1}{gv^2 E} \partial_z (v\lambda) \rightarrow \frac{1}{gEv} \partial_z \lambda$ outside of the wall. Using the expression for reflection and transmission coefficients from eq. (102)

$$r_k^\lambda = \frac{\tilde{v}^2 k^z - v^2 \tilde{k}^z}{\tilde{v}^2 k^z + v^2 \tilde{k}^z} , \quad t_k^\lambda = \frac{2k^z v \tilde{v}}{\tilde{v}^2 k^z + v^2 \tilde{k}^z} , \quad (170)$$

we can compute the amplitude for the processes $J^\mu \rightarrow \chi_\lambda^\mu$ corresponding to the interaction $J_\mu \chi_\lambda^\mu$. The computation goes as follows

$$\mathcal{M} = \frac{k^z}{gEv} \frac{(p+q)_\mu k^\mu}{\Delta p} - \frac{k^z}{gEv} r_k^\lambda \frac{(p+q)_\mu k_r^\mu}{\Delta p_r} - \frac{\tilde{k}^z}{gE\tilde{v}} t_k^\lambda \frac{(p+q)_\mu \tilde{k}^\mu}{\Delta \tilde{p}}$$

$$= \frac{(p+q)_z}{E} \underbrace{\left(\frac{k^z}{gv} - \frac{k^z}{gv} r_k^\lambda - \frac{\tilde{k}^z}{g\tilde{v}} t_k^\lambda \right)}_{=0} = 0 , \quad (171)$$

the last expression in brackets is the matching condition for the λ field (eq. (99)) which must be satisfied. Note that terms cancelling each other in the brackets are growing in energy, which makes crucially important the calculation of exact values of reflection and transmission coefficients.

C WKB regime in the case of current non-conservation

In the main text we focus only on the transition radiation from the conserved current. How we can perform a similar calculation in the case when the current is not conserved? Let us consider the following example with scalar fields

$$\mathcal{L} = -\frac{1}{4}F_{\mu\nu}F^{\mu\nu} + |D_\mu H|^2 - V(|H|) + |D_\mu\phi|^2 - m_\psi^2|\phi|^2 + (\kappa\phi^2 H + h.c.). \quad (172)$$

The charges under the gauged $U(1)$ symmetry are as follows: $Q_{U(1)}(H) = 1, Q_{U(1)}(\phi) = -1/2$. In the section 3.5, in order to perform the WKB calculation and get rid of interactions that can potentially lead to the divergences we have used the current conservation equations to modify the expression for the matrix elements. In the case of the system in eq. (172) the divergence of the current becomes equal to:

$$\partial_\mu J_\phi^\mu = \sqrt{2}v(z) (\kappa^* \phi^{*2} - \kappa\phi^2), \quad J_\phi^\mu = i(\phi^* \partial^\mu \phi - \phi \partial^\mu \phi^*). \quad (173)$$

The interaction between the λ polarisation and J_ϕ^μ and can be written as follows:

$$gQ_\phi J_\phi^\mu A_\mu^{(\lambda)} \rightarrow Q_\phi \left[-\sqrt{2} (\kappa^* \phi^{*2} - \kappa\phi^2) \frac{1}{Ev(z)} \partial_z (v(z)\lambda(z)) - \frac{g^2 v(z)}{E} \lambda(z) J_z \right]. \quad (174)$$

We can see that on top of the term λJ_z present in the conserved current case, there is an additional interaction. However, this interaction is not growing with energy, and in the limit $v(z) \rightarrow 0$, it is finite (see discussion in the appendix D), thus the calculation of the vector emission becomes straightforward.

D Properties of the potential for λ field

In the main text we have shown that λ field satisfies the following equation of motion eq. (81)–(82)

$$\begin{aligned} (-E^2 - \partial_z^2 + U_\lambda(z)) \lambda &= 0, \\ U_\lambda(z) &= g^2 v^2(z) + 2 \left(\frac{\partial_z v}{v} \right)^2 - \frac{\partial_z^2 v}{v}. \end{aligned} \quad (175)$$

Let us investigate the properties of the function U_{λ_z} .

Broken \rightarrow Broken In this case

$$v_{z \rightarrow \pm\infty} \neq 0, \quad (176)$$

and the potential has the limits :

$$U_\lambda(z)|_{z \rightarrow \pm\infty} = g^2 v^2(z \rightarrow \pm\infty), \quad (177)$$

where we have used that $v', v'' \rightarrow 0$ outside of the wall. Physics wise this result is expected since λ mode must have the mass of the vector gv outside of the wall.

Symmetric→**Broken** Here we will assume

$$v(z \rightarrow -\infty) = 0, \quad v(z \rightarrow \infty) = \tilde{v} \neq 0. \quad (178)$$

On the broken side as expected

$$U_\lambda(z \rightarrow \infty) = g^2 v^2(z \rightarrow \infty) = g^2 \tilde{v}^2, \quad (179)$$

the potential becomes equal to the mass square of the vector boson. To find its limit on the symmetric side we need to look at the equation defining $v(z)$:

$$\partial_z^2 v(z) = V'(v(z)), \quad (180)$$

where the prime stands for a derivative with respect to $v(z)$. Integrating this equation we get

$$\frac{1}{2} (\partial_z v(z))^2 = V(v(z)) - C, \quad (181)$$

where $C = -(\partial_z v(z_0))^2 + V(v(z_0))$ is a ‘constant of integration’. We can choose $z_0 \rightarrow -\infty$, then using $v', v \rightarrow 0$ we get $C = V(v(-\infty)) = V(0)$, which need not be zero. Now we look at the limits as $z \rightarrow -\infty$. At this point, using eqs. (180) and (181) we can write the various terms of the U_λ function in terms of the potential V and its derivatives V' :

$$\begin{aligned} \frac{\partial_z^2 v(z)}{v(z)} &= \frac{\partial_z^2 v}{v} = \frac{V'(v)}{v} \xrightarrow{v \rightarrow 0} V''(0), \\ \left(\frac{\partial_z v(z)}{v(z)} \right)^2 &= \left(\frac{\partial_z v}{v} \right)^2 = 2 \frac{V(v) - V(0)}{v^2} \xrightarrow{v \rightarrow 0} V''(0). \end{aligned} \quad (182)$$

However, in the limit $z \rightarrow -\infty, v \rightarrow 0$, we know that the first derivative of the potential V must be equal to zero at this point

$$\left. \frac{\partial V}{\partial v} \right|_{v \rightarrow 0} = 0, \quad (183)$$

since there is a local minimum at $v = 0$. Thus in the region $v \rightarrow 0$ we can write down:

$$\begin{aligned} V(v)|_{v \rightarrow 0} &= \frac{V''(0)v^2}{2} + V(0) \Rightarrow \\ \left. \frac{V'(v)}{v} \right|_{v \rightarrow 0} &= V''(0), \quad 2 \frac{V(v) - V(0)}{v^2} = V''(0). \end{aligned} \quad (184)$$

Combining these results we can see that

$$\lim_{z \rightarrow -\infty} U_\lambda(z) = V''(0) = m_{h,s}^2, \quad (185)$$

where $m_{h,s}$ is the mass of the scalar on the symmetric side. We can see that as was discussed in the section 3.2 U_λ has the correct properties for a potential of a d.o.f interpolating between the scalar field and λ polarisation on different sides of the wall.

E Evaluation of phase space Integrals

In this appendix, we provide some details regarding the evaluation of the phase space integrals, and how to derive analytical expressions. We will always be interested in the limit of large incoming energy $p^0 \gg$ all masses. The types of integrals we deal with are all of the form

$$I(p^0) = \int_{\text{const}}^{l_1(p^0)} dk \int_{\text{const}'}^{l_2(p^0, k)} dk_{\perp}^2 \text{Int}(p^0, k, k_{\perp}^2), \quad (186)$$

where the dependence on couplings and masses m_i is implicit. When $I(p^0)$ admits an expansion around infinity, this can be obtained in principle straightforwardly as

$$I(p^0) = I(1/x)|_{x \rightarrow 0} + \frac{d}{dx} I(1/x) \Big|_{x \rightarrow 0} \frac{1}{p^0} + \dots \quad (187)$$

and one can sometimes take this ‘exact’ approach. However, such an expansion does not always exist²⁵, or if it does, its coefficients might in practice be difficult to evaluate. Moreover, in the presence of large mass hierarchies, the regime where eq. (187) is actually a good approximation can begin at arbitrarily high energies²⁶. One can often successfully use a different expansion instead, which we call ‘collinear expansion’, of $p^0, k^z \gg k_{\perp}, m_i$ where m_i stands for all masses. Keeping the leading term, reduces integrands to the form

$$\text{Int}(p^0, k, k_{\perp}^2) = \frac{N(k, k_{\perp}, m_i)}{[(k_{\perp, m}^{IR})^2 + k_{\perp}^2]^2} \quad \text{for } p^0, k^z \gg k_{\perp}, m_i, \quad (188)$$

where

$$k_{\perp}^2 \lesssim (k_{\perp, m}^{IR})^2 \equiv \frac{k_z^2 m_{\psi}^2 - k^z m^2 p_0}{(p_0)^2} + m^2 > 0. \quad (189)$$

The function N depends on the contribution in question but we wish to highlight the factor in denominator. This form makes most manifest the properties of the phase space structure in particular for τ polarisation (and scalars), most importantly when m (and possibly m_{ψ}) is very small. For a given k^z , the integrand is peaked for $k_{\perp}^2 \lesssim (k_{\perp, m}^{IR})^2$. Notice the role of $k_{\perp, m}^{IR}$ - its presence regulates an otherwise logarithmically IR divergent integral. Indeed the momentum transfer diverges in the limit of $m, m_{\psi} \rightarrow 0$. It is easy to prove that $k_{\perp, m}^{IR} < k^z$ for small m , justifying the expansion. When m/m_{ψ} is very small, clearly there are two relativistic regimes, the first given by

$$p^0 \lesssim k^z m_{\psi} / m, \quad (190)$$

where k^z should be taken in the dominant region. Typically $k^z \sim \tilde{m}$ for step function contributions and $\sim L_w^{-1}$ for WKB. Above this scale instead one reaches the true asymptotic behaviour where eq. (187) is valid.

²⁵For example, in vector emission in symmetry breaking transitions, for $m = 0$ we find logarithmic growth.

²⁶We saw this for example when there are large scale other than p^0 such as $\tilde{m} m_{\psi} / m$ in plots in the main text figs. 3, 5, 7 and 8.

E.1 Scalars

Scalar R -mover emission (WKB) We begin with the most dominant contribution to scalar emission at the highest of energies $p^0 \rightarrow \infty$. The amplitude is the simplest that one can encounter,

$$\mathcal{M}_R^{\text{wkb}} = \left(\frac{y}{i\Delta p} + \frac{\tilde{y}}{-i\Delta \tilde{p}} \right), \quad (191)$$

and

$$\langle \Delta p_R^{\text{wkb}} \rangle = \int_{L_w^{-1}}^{k_{\text{max}}^z} dk^z \int_0^{k_{\perp, \text{cut}}^2} \frac{dk_{\perp}^2}{2} \frac{|\mathcal{M}_R^{\text{wkb}}|^2}{(2\pi)^2 8p^z q^z k_0} \Delta p_R. \quad (192)$$

For $m \neq 0$, properly evaluating the expansion eq. (187) for this case is tricky²⁷. However, the collinear expansion eq. (188) works extremely well, giving

$$\langle \Delta p_R^{\text{wkb}} \rangle \approx \frac{y^2 \Delta m^4}{32\pi^2} \int_{L_w^{-1}}^{k_{\text{max}}^z} dk^z \int_0^{k_{\perp, \text{cut}}^2} dk_{\perp}^2 \frac{(k^z - p_0)^2 / (p_0)^4}{[(k_{\perp, m}^{IR})^2 + k_{\perp}^2]^2 [(k_{\perp, \tilde{m}}^{IR})^2 + k_{\perp}^2]}, \quad (193)$$

where k_{\perp}^{IR} is given by eq. (189). We see indeed that for large p^0 the integrand is relatively flat in k^z while k_{\perp} is strongly IR dominated as anticipated in the preamble above, justifying the expansion. The integrals can now be computed exactly and we obtain eq. (51). We can see clearly however that there is also an intermediate regime for small m/m_{ψ} characterised by a plateau:

$$\langle \Delta p_R^{\text{wkb}} \rangle \approx \begin{cases} \frac{y^2 \tilde{m}^2 L_w}{32\pi^2 m_{\psi}^2}, & L_w^{-1} \ll p^0 \lesssim L_w^{-1} \frac{m_{\psi}}{m} \\ \text{eq. (51)}, & p^0 \gtrsim L_w^{-1} \frac{m_{\psi}}{m} \end{cases}, \quad (194)$$

where we remind ourselves that there is no WKB contribution at all unless we can emit modes greater than the inverse wall length. The value of the plateau is easily obtained by setting $m = 0$ at the start and computing the leading order in eq. (187). However, in this regime, we find the step function contributions are more important and we move on there now.

Scalar R and L -mover emission (step wall) The step wall case is an interesting theory exercise in its own right, since everything can be done exactly. For scalars the contributions are

$$\langle \Delta p_R^{\text{step}} \rangle = \int_{\Delta m}^{L_w^{-1}} dk^z \int_0^{k_{\perp, \text{max}}^2} \frac{dk_{\perp}^2}{2} \frac{|\mathcal{M}_R^{\text{step}}|^2}{(2\pi)^2 8p^z q^z k_0} \Delta p_R. \quad (195)$$

$$\langle \Delta p_L^{\text{step}} \rangle = \int_0^{L_w^{-1}} dk^z \int_0^{k_{\perp, \text{max}}^2} \frac{dk_{\perp}^2}{2} \frac{|\mathcal{M}_L^{\text{step}}|^2}{(2\pi)^2 8p^z q^z k_0} \Delta p_L. \quad (196)$$

²⁷The coefficient of the $1/p^0$ term in eq. (187) is the first non-zero contribution as expected from fig. 5. Out of the three terms to evaluate only one is non-zero in the $x \rightarrow 0$ limit. Said limit cannot be taken before the integral is evaluated however and such a task proves unnecessarily difficult.

where the matrix elements are given by eqs. (29) and (30). Evaluating these in the asymptotic limit we obtain

$$\langle \Delta p_L^{\text{step}} \rangle \approx \frac{y^2 \tilde{m}}{32\pi^2 m_\psi^2} \begin{cases} 4, & p_0 \lesssim \tilde{m} m_\psi / m \\ \frac{4m_\psi^2 \Delta m}{3\tilde{m} m^2 p_0^2} \left[m^2 \left(\ln \frac{m^2}{\tilde{m}^2} - 1 \right) + \tilde{m}^2 \right], & p_0 \gtrsim \tilde{m} m_\psi / m \end{cases} \quad (197)$$

$$\langle \Delta p_R^{\text{step}} \rangle \approx \frac{y^2 \tilde{m}}{32\pi^2 m_\psi^2} \begin{cases} 1 - \tilde{m} L_w, & p_0 \lesssim 4 \tilde{m} m_\psi / m \\ \frac{m_\psi^2 (L_w^{-1} - \Delta m)}{4\tilde{m} m^2 p_0^2} \left[\Delta m^2 + 2m^2 \ln \left(\frac{m}{\tilde{m}} \right) \right], & p_0 \gtrsim L_w^{-1} m_\psi / m \end{cases} \quad (198)$$

For the R -contribution there is an intermediate regime well approximated by the WKB asymptotic formula in (51), as can be seen from fig. 5 (bottom right panel).

E.2 Vectors: τ emission

The three relevant amplitudes are repeated here again

$$\begin{aligned} \mathcal{M}_{\tau,L}^{\text{step}} &= -ig \epsilon_{\tau_2}^\mu (p+q)_\mu \left(\frac{1}{\Delta p_r} + \frac{r_{\tau,k}}{\Delta p} + \frac{t_{\tau,k}}{-\Delta \tilde{p}_r} \right), \\ \mathcal{M}_{\tau,R}^{\text{step}} &= -ig \sqrt{\frac{k^z}{\tilde{k}^z}} \epsilon_{\tau_2}^\mu (p+q)_\mu \left[\frac{\tilde{k}^z t_k}{k^z \Delta p} - \frac{1}{\Delta \tilde{p}} + \frac{r_k}{\Delta \tilde{p}_r} \right], \\ \mathcal{M}_\tau^{\text{wkb}} &= -ig \epsilon_{\tau_2}^\mu (p+q)_\mu \left(\frac{1}{\Delta p_r} + \frac{1}{-\Delta \tilde{p}} \right). \end{aligned} \quad (199)$$

For τ polarisation we can treat both types of transitions of interest at the same time by interpreting the m, \tilde{m} correctly.

E.3 $m \neq 0$ asymptotic p^0 regime

We present now the dominant contribution $\mathcal{M}_{\tau,L}^{\text{step}}$ in detail ²⁸. The amplitude squared is

$$|\mathcal{M}_{\tau,L}^{\text{step}}|^2 = \frac{16g^2 k_z^2 k_\perp^2 p_0^2}{(k_z^2 + m^2)(k_z^2 - (p^z - q^z)^2)^2} \begin{cases} \frac{\Delta m^2}{\Delta m^2 - k_z^2 + (p^z - q^z)^2}, & k^z < \Delta m \\ \frac{(k^z - \tilde{k}^z)^2}{(\tilde{k}^z + p^z - q^z)^2}, & k^z > \Delta m \end{cases}, \quad (200)$$

where, as usual, we make a distinction between two branches distinguished by \tilde{k} being imaginary or real. We can explicitly evaluate the leading term in the large p^0 expansion eq. (187) for the total momentum exchanged. We report only the first, dominant, branch

$$\langle \Delta p_L^{\tau,\text{step}} \rangle \longrightarrow \frac{g^2 \tilde{m}}{8\pi^2} F_{\tau,L}^{\text{step}}(r \equiv \tilde{m}/m), \quad k^z < \Delta m \quad \text{branch}, \quad (201)$$

²⁸Similar asymptotic expressions can be derived for all contributions but we do not believe it useful to fill the paper with multiple complicated formulae. We deem the total fitted formulae in the main text of more practical use given the overall uncertainties in the physics of FOPTs in the early universe.

where the dimensionless function defined is

$$F_{\tau,L}^{\text{step}}(r) = \frac{1}{(r^2 - 1)} \left\{ 2 \left(\pi(1+r)^2 - (1+r^2) \csc^{-1}[r] \right) \ln[r - \sqrt{r^2 - 1}] - 2 \tan^{-1}[\sqrt{r^2 - 1}] \right. \\ \left. - 4(1+r)^2 \left(G - \Im \text{Li}_2 \left[i(r + \sqrt{r^2 - 1}) \right] \right) - 2(r^2 - 1)(r - 1 + \sqrt{r^2 - 1}) + 2\pi r \cosh^{-1}[r] \right. \\ \left. - r^2 \left(8\sqrt{r^2 - 1} \coth^{-1} \left[1 - \frac{2r}{\sqrt{r^2 - 1}} \right] + \tan^{-1}[\sqrt{r^2 - 1}] (4\sqrt{r^2 - 1} + 4 \log[r] - 2) \right) \right\} .$$

$G \approx 0.916$ is Catalan's constant and \Im stands for imaginary part. We caution the reader that, while the analytical evaluation of integrals is a fun endeavour, we believe that, at least at the present time, the numerical fits presented in the main text are more useful.

E.4 The $m \rightarrow 0$ regime

The inter-relativistic regime of growth $\propto \log(p_0)$ discussed in the main text when $m/m_\psi \ll 1$ can be found analytically by simply setting $m = 0$, keeping $m_\psi \neq 0$, and using the collinear expansion eq. (188) to evaluate the phase space integrals. We obtain

$$\langle \Delta p_L^{\tau, \text{step}} \rangle \simeq \frac{g^2 \tilde{m}}{2\pi^2} \left(1 + 2 \ln \left(\frac{p_0}{m_\psi} \right) \right), \quad (202)$$

$$\langle \Delta p_R^{\tau, \text{step}} \rangle \simeq \frac{g^2 \tilde{m}}{1800\pi^2} \left[526 - 900G - 195\pi + 480 \ln \left(\frac{\sqrt{2}p_0}{m_\psi} \right) \right] \\ + \frac{g^2 \tilde{m}^2 L_w}{8\pi^2} \left[3 - 2 \ln \left(\frac{\tilde{m} L_w p_0}{m_\psi} \right) \right] + \mathcal{O}((\tilde{m}L)^2), \quad (203)$$

$$\langle \Delta p_R^{\tau, \text{wkb}} \rangle \simeq \frac{g^2 \tilde{m}^2 L_w}{8\pi^2} \left[2 \ln \left(\frac{\tilde{m} L_w p_0}{m_\psi} \right) - 3 \right], \quad (204)$$

where $G \approx 0.916$ is Catalan's constant. The total contribution is dominated by L emission and then scales like

$$\langle \Delta p^{\tau, \text{tot}} \rangle \simeq \langle \Delta p_L^{\tau, \text{step}} \rangle \simeq \frac{g^2 \tilde{m}}{2\pi^2} \left(1 + 2 \ln \left(\frac{p_0}{m_\psi} \right) \right). \quad (205)$$

We remind the reader that these are the results for the single vector emission, to the expression above cannot be trusted for the large values of the log.

E.5 Vectors: λ emission

We report again the relevant amplitudes here with general $v \neq 0$:

$$\mathcal{M}_{\lambda,L}^{\text{step}} = -i \frac{g}{E} (p^z + q^z) \left[gv \left(\frac{1}{\Delta p_r} + \frac{r_k^\lambda}{\Delta p} \right) - g\tilde{v} \frac{t_k^\lambda}{\Delta \tilde{p}_r} \right], \quad (206)$$

$$\mathcal{M}_{\lambda,R}^{\text{step}} = -i \frac{g}{E} (p^z + q^z) \sqrt{\frac{k^z}{\tilde{k}^z}} \left[gv \frac{\tilde{k}^z}{k^z} \frac{t_k^\lambda}{\Delta p} - g\tilde{v} \left(\frac{1}{\Delta \tilde{p}} - \frac{r_k^\lambda}{\Delta \tilde{p}_r} \right) \right], \quad (207)$$

$$\mathcal{M}_\lambda^{\text{wkb red.}} = -i \frac{g}{E} (p^z + q^z) \left[\frac{gv}{\Delta p} - \frac{g\tilde{v}}{\Delta \tilde{p}} \right]. \quad (208)$$

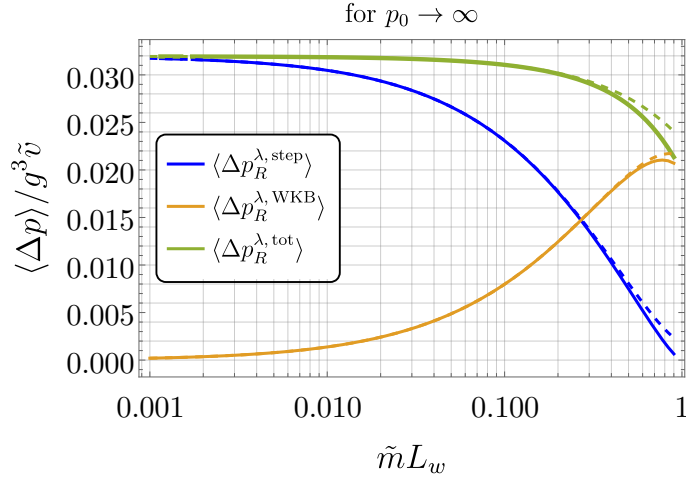


Figure 10: Analytically derived exact formulae for the exchanged momentum in the asymptotic limit $p^0 \rightarrow \infty$ from the emission of λ polarisations. Dashed lines correspond to the small $\tilde{m}L_w$ approximations reported in eq. (209). The sum of the two different contributions is roughly constant.

Unlike the case of τ we must consider the two transitions of interest separately.

Symmetric to Broken ($v = 0$): The symmetric side mass of the λ degree of freedom is $m_{h,s}$ – the mass of the Higgs in that phase. We find however that taking $m_{h,s} = 0$ incurs an error which is at most $\sim 10\%$ when $m_{h,s} \sim \text{few} \times \tilde{m}$. One can rigorously prove that in the limit $p^0 \rightarrow \infty$ we have

$$\begin{aligned}
 \langle \Delta p_R^{\lambda, \text{step}} \rangle &\longrightarrow \frac{g^4 \tilde{v}^2}{8\pi^2 \tilde{m}} F_{\lambda, R}^{\text{step}}(\tilde{m}L_w) & (209) \\
 &= \frac{g^4 \tilde{v}^2}{8\pi^2 \tilde{m}} [2 + 4G - \pi + \tilde{m}L_w (2 \ln(\tilde{m}L_w) - 2 \ln(2) - 1)] + \mathcal{O}((\tilde{m}L_w)^3) , \\
 \langle \Delta p_R^{\lambda, \text{wkb}} \rangle &\longrightarrow \frac{g^4 \tilde{v}^2}{8\pi^2 \tilde{m}} \left[\tan^{-1} \left(\frac{\tilde{m}L_w}{\sqrt{1 - \tilde{m}^2 L_w^2}} \right) - \tilde{m}L_w \ln \left(1 - \sqrt{1 - \tilde{m}^2 L_w^2} \right) \right] , & (210)
 \end{aligned}$$

where $G \approx 0.916$ is Catalan’s constant. $F_{\lambda, R}^{\text{step}}$ has a closed form in terms of (hyperbolic) trig functions and the dilogarithm, but we have deemed it more useful to explicitly report only its small $\tilde{m}L_w$ limit - an excellent approximation, as can be seen in fig. 10. There we also see that the sum of the two contributions is roughly constant, giving

$$\langle \Delta p^{\lambda, \text{total}} \rangle \approx \langle \Delta p_R^{\lambda, \text{step}} \rangle + \langle \Delta p_R^{\lambda, \text{wkb}} \rangle \simeq \frac{g^4 v^2}{8\pi^2 \tilde{m}} [2 + 4G - \pi - \tilde{m}L_w \ln(2)] , \quad (211)$$

to leading orders in $\tilde{m}L_w$. A more accurate expression when $\tilde{m}L_w \sim 1$ is eq. (210).

F Pressure in the EW phase transition

In this work, we computed the pressure in the context of an Abelian toy model, where the $U(1)$ gauge boson was emitted by a complex scalar. Emission from fermions will not significantly change our result per degree of freedom. Moreover, the emission can be straightforwardly expanded to the non-Abelian case.

For the SM case, the pressure at $1 \rightarrow 2$ level originates from the vertices inducing $\psi \rightarrow Z\psi$ (where the first particle in the final state is soft and ψ is some fermion of the SM), $\psi \rightarrow W^\pm\psi$ for the gauge bosons emitted from fermions $H \rightarrow W^\pm H$, $H \rightarrow ZH$ for the gauge bosons emitted from the Higgs and $A \rightarrow WW$, $W \rightarrow WA$, $Z \rightarrow WW$, $W \rightarrow WZ$, $W \rightarrow ZW$ for gauge bosons emitting gauge bosons. The careful counting of all the processes involved in the pressure was presented in Appendix C of [45]. This leads to a final pressure of the form

$$\mathcal{P}_{\text{SM},1\rightarrow 2} \approx 157 \times \alpha_{\text{em}} M_Z \frac{4\gamma_w \zeta(3) T^3}{\pi} \left[0.135 \log \left(\frac{\tilde{v}}{T} + 2.26 \right) - 0.085 - 0.2 \frac{\log \left(\frac{\tilde{v}}{T} + 2.26 \right)}{\tilde{v}/T} + \frac{0.19}{\tilde{v}/T} \right], \quad (212)$$

where every contribution is normalised to the fine structure constant α_{em} and the Z boson mass M_Z in the broken phase. We caution the reader that this expression is still an estimate and may incur future revision, for example, from a better understanding of finite temperature corrections - see section 4.2.

G Sensitivity to wall width

In this work we separated the phase space of particles according to when the step wall and WKB approximations are justified

- $k^z < L_w^{-1}$, Step wall
- $k^z > L_w^{-1}$, WKB

where L_w is the width of the wall. However, this is a somewhat arbitrary quantity, significant up to some order 1 factor. Although we have discussed the sensitivity of our results to L_w in several places, we summarise it in this dedicated appendix.

We study numerically how pressure changes with wall width. For scalars, the dominant contribution comes from the WKB regime and dependence on L_w vanishes, as can be seen explicitly by the analytical formulae eqs. (51) and (197). The results for vector emission are highlighted in fig. 11. The left and right columns show left and right mover emission respectively, while top and lower panels correspond to τ and λ polarisations. The first thing to notice is that $\langle \Delta p_L^{\tau, \text{step}} \rangle$, which is the dominant contribution for super-cooled symmetric to broken transitions is largely insensitive to L_w . Secondly, $\langle \Delta p_R^{\lambda, \text{step}} \rangle$ and $\langle \Delta p_R^{\lambda, \text{wkb}} \rangle$ show almost linear dependence around $L_w \sim \text{few } \tilde{m}$ but their *sum* is largely constant. This point was made also in fig. 10 using analytical asymptotic formulae. Instead, $\langle \Delta p_L^{\lambda, \text{step}} \rangle$, which exists only in broken to broken transitions is linearly dependent on the cut-off (see eq. (142)).

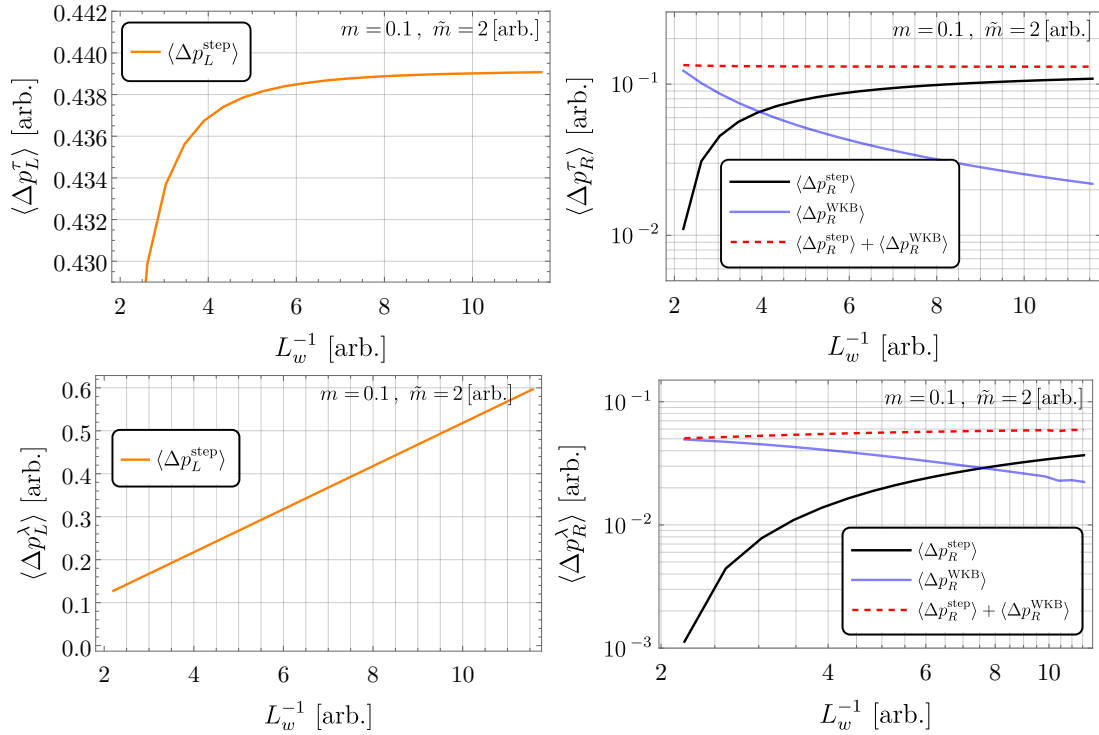


Figure 11: Dependence of various contributions to average momentum transfer, due to the emission of a vector boson, on the inverse wall width L_w^{-1} in the limit $p_0 \rightarrow \infty$. Top (Bottom) panels refer to τ (λ) emission, while left (right) column refers to L (R) emission. In this limit, any dependence on the mass of the emitter (m_ψ) vanishes.

H The suppressed region $\Delta p_z L_w \gg 1$: the Fourier constraint

In section 2.6 and afterward, we stated that in WKB approximation the region $\Delta p_z L_w \gg 1$ should have a very suppressed contribution to the pressure. In this appendix, we bring some arguments to this claim (see also Appendix B.1 of [66] and Section V of [63] for previous discussion). The function that we have to study is typically the following integral

$$\mathcal{M} \approx \int_{-\infty}^{\infty} dz V(z) e^{i \int_{-\infty}^z \Delta p_z(z') dz'} , \quad (213)$$

where far from the wall both $\Delta p(z)$ and $V(z)$ are constant. In this case, we can always absorb $V(z) = V_0 \exp[\int_0^z (V'/V) dz]$ inside the exponent (redefining Δp) and thus we can focus only on the integrals where $V(z) = V_0$

$$\mathcal{M} \approx V_0 \int_{-\infty}^{\infty} dz e^{i \int_0^z \Delta p_z(z') dz'} . \quad (214)$$

In general, these integrals must be evaluated numerically for various wall shapes. However, for particular choices like

$$\Delta p_z(z) = \Delta p_z + \frac{\epsilon}{2} \tanh z/L_w , \quad (215)$$

we can evaluate the integrals analytically. In eq. (215), ϵ parameterises the change of the phase across the wall. This leads to

$$\mathcal{M} = V_0 \int_{-\infty}^{\infty} dz \exp [i \Delta p_z z + i \epsilon f(z)] , \quad (216)$$

$$f(z) = \frac{L_w}{2} \log \cosh \frac{z}{L_w} , \quad (217)$$

and give finally

$$|\mathcal{M}|^2 = \frac{\pi \epsilon L_w |V_0|^2}{2 \Delta p_z^2 - \epsilon^2/2} \times \frac{\sinh(\pi \epsilon L_w/2)}{\sinh(\pi(\Delta p_z - \epsilon/2)L_w/2) \sinh(\pi(\Delta p_z + \epsilon/2)L_w/2)} \quad (218)$$

$$\approx \frac{\pi \epsilon L_w |V_0|^2}{2 \Delta p_z^2} \times \frac{\sinh(\pi \epsilon L_w/2)}{\sinh^2(\pi \Delta p_z L_w/2)} . \quad (219)$$

For $\epsilon L_w \lesssim 1$, $\Delta p_z L_w \gg 1$, we obtain

$$|\mathcal{M}|^2 \approx \frac{\pi \epsilon L_w |V_0|^2}{4 \Delta p_z^2} \times \pi \epsilon L_w e^{-\pi \Delta p_z L_w} = \frac{(\pi \epsilon L_w)^2 |V_0|^2}{4 \Delta p_z^2} \times e^{-\pi \Delta p_z L_w} \quad (220)$$

which shows that $|\mathcal{M}|^2 \propto e^{-\pi \Delta p_z L_w}$ and then decay exponentially with $\Delta p_z L_w \gg 1$. We have also checked numerically the behaviour of the amplitude for other wall shapes, with a similar behaviour (for example Erf function) and always find exponential suppression.

References

- [1] D. A. Kirzhnits and A. D. Linde *Phys. Lett. 42B: No. 4, 471-4(25 Dec 1972)*. (1, 1972).
- [2] S. Weinberg *Phys. Rev. D* **9** (Jun, 1974) 3357–3378.
- [3] E. Witten *Phys. Rev.* **D30** (1984) 272–285.
- [4] C. Bonati, M. D’Elia, P. de Forcrand, O. Philipsen, and F. Sanfilippo *PoS LATTICE2013* (2014) 219, [[arXiv:1311.0473](#)].
- [5] M. Laine and K. Rummukainen *Nucl. Phys. B Proc. Suppl.* **73** (1999) 180–185, [[hep-lat/9809045](#)].
- [6] G. Degrassi, S. Di Vita, J. Elias-Miro, J. R. Espinosa, G. F. Giudice, G. Isidori, and A. Strumia *JHEP* **08** (2012) 098, [[arXiv:1205.6497](#)].
- [7] V. A. Kuzmin, V. A. Rubakov, and M. E. Shaposhnikov *Phys. Lett. B* **155** (1985) 36.
- [8] M. Shaposhnikov *JETP Lett.* **44** (1986) 465–468.
- [9] A. E. Nelson, D. B. Kaplan, and A. G. Cohen *Nucl. Phys. B* **373** (1992) 453–478.
- [10] M. Carena, M. Quiros, and C. E. M. Wagner *Phys. Lett. B* **380** (1996) 81–91, [[hep-ph/9603420](#)].
- [11] J. M. Cline *Phil. Trans. Roy. Soc. Lond. A* **376** (2018), no. 2114 20170116, [[arXiv:1704.08911](#)].
- [12] A. J. Long, A. Tesi, and L.-T. Wang *JHEP* **10** (2017) 095, [[arXiv:1703.04902](#)].
- [13] S. Bruggisser, B. Von Harling, O. Matsedonskyi, and G. Servant *JHEP* **12** (2018) 099, [[arXiv:1804.07314](#)].
- [14] S. Bruggisser, B. Von Harling, O. Matsedonskyi, and G. Servant *Phys. Rev. Lett.* **121** (2018), no. 13 131801, [[arXiv:1803.08546](#)].
- [15] D. E. Morrissey and M. J. Ramsey-Musolf *New J. Phys.* **14** (2012) 125003, [[arXiv:1206.2942](#)].
- [16] A. Azatov, M. Vanvlasselaer, and W. Yin *JHEP* **10** (2021) 043, [[arXiv:2106.14913](#)].
- [17] I. Baldes, S. Blasi, A. Mariotti, A. Sevrin, and K. Turbang [arXiv:2106.15602](#).
- [18] E. J. Chun, T. P. Dutka, T. H. Jung, X. Nagels, and M. Vanvlasselaer [arXiv:2305.10759](#).
- [19] A. Falkowski and J. M. No *JHEP* **02** (2013) 034, [[arXiv:1211.5615](#)].
- [20] I. Baldes, Y. Gouttenoire, and F. Sala *JHEP* **04** (2021) 278, [[arXiv:2007.08440](#)].
- [21] A. Azatov, M. Vanvlasselaer, and W. Yin *JHEP* **03** (2021) 288, [[arXiv:2101.05721](#)].
- [22] I. Baldes, Y. Gouttenoire, F. Sala, and G. Servant *JHEP* **07** (2022) 084, [[arXiv:2110.13926](#)].
- [23] P. Asadi, E. D. Kramer, E. Kuflik, G. W. Ridgway, T. R. Slatyer, and J. Smirnov *Phys. Rev. D* **104** (2021), no. 9 095013, [[arXiv:2103.09827](#)].
- [24] I. Baldes, Y. Gouttenoire, and F. Sala *SciPost Phys.* **14** (2023) 033, [[arXiv:2207.05096](#)].
- [25] I. Baldes, M. Dichtl, Y. Gouttenoire, and F. Sala [arXiv:2306.15555](#).
- [26] H. Kodama, M. Sasaki, and K. Sato *Progress of Theoretical Physics* **68** (12, 1982) 1979–1998, [<https://academic.oup.com/ptp/article-pdf/68/6/1979/5311817/68-6-1979.pdf>].
- [27] K. Kawana and K.-P. Xie *Phys. Lett. B* **824** (2022) 136791, [[arXiv:2106.00111](#)].
- [28] T. H. Jung and T. Okui [arXiv:2110.04271](#).
- [29] Y. Gouttenoire and T. Volansky [arXiv:2305.04942](#).

- [30] M. Lewicki, P. Toczec, and V. Vaskonen [arXiv:2305.04924](#).
- [31] C. J. Hogan *Mon. Not. Roy. Astron. Soc.* **218** (1986) 629–636.
- [32] A. Kosowsky and M. S. Turner *Phys. Rev.* **D47** (1993) 4372–4391, [[astro-ph/9211004](#)].
- [33] A. Kosowsky, M. S. Turner, and R. Watkins *Phys. Rev. Lett.* **69** (1992) 2026–2029.
- [34] M. Kamionkowski, A. Kosowsky, and M. S. Turner *Phys. Rev.* **D49** (1994) 2837–2851, [[astro-ph/9310044](#)].
- [35] C. Grojean, G. Servant, and J. D. Wells *Phys. Rev. D* **71** (2005) 036001, [[hep-ph/0407019](#)].
- [36] C. Delaunay, C. Grojean, and J. D. Wells *JHEP* **04** (2008) 029, [[arXiv:0711.2511](#)].
- [37] J. Ellis, M. Lewicki, and J. M. No [arXiv:1809.08242](#). [*JCAP*1904,003(2019)].
- [38] J. Ellis, M. Lewicki, J. M. No, and V. Vaskonen *JCAP* **1906** (2019), no. 06 024, [[arXiv:1903.09642](#)].
- [39] J. R. Espinosa and M. Quiros *Phys. Rev. D* **76** (2007) 076004, [[hep-ph/0701145](#)].
- [40] A. Beniwal, M. Lewicki, J. D. Wells, M. White, and A. G. Williams *JHEP* **08** (2017) 108, [[arXiv:1702.06124](#)].
- [41] V. Barger, P. Langacker, M. McCaskey, M. J. Ramsey-Musolf, and G. Shaughnessy *Phys. Rev. D* **77** (2008) 035005, [[arXiv:0706.4311](#)].
- [42] J. R. Espinosa, T. Konstandin, and F. Riva *Nucl. Phys. B* **854** (2012) 592–630, [[arXiv:1107.5441](#)].
- [43] J. Kozaczuk, M. J. Ramsey-Musolf, and J. Shelton *Phys. Rev. D* **101** (2020), no. 11 115035, [[arXiv:1911.10210](#)].
- [44] G. Kurup and M. Perelstein *Phys. Rev. D* **96** (2017), no. 1 015036, [[arXiv:1704.03381](#)].
- [45] A. Azatov, G. Barni, S. Chakraborty, M. Vanvlasselaer, and W. Yin *JHEP* **10** (2022) 017, [[arXiv:2207.02230](#)].
- [46] I. Garcia Garcia, S. Krippendorf, and J. March-Russell *Phys. Lett. B* **779** (2018) 348–352, [[arXiv:1607.06813](#)].
- [47] J. R. Espinosa, T. Konstandin, J. M. No, and G. Servant *JCAP* **1006** (2010) 028, [[arXiv:1004.4187](#)].
- [48] R. Jinno and M. Takimoto *JCAP* **1901** (2019) 060, [[arXiv:1707.03111](#)].
- [49] M. Fairbairn, E. Hardy, and A. Wickens *JHEP* **07** (2019) 044, [[arXiv:1901.11038](#)].
- [50] M. Breitbach, J. Kopp, E. Madge, T. Opferkuch, and P. Schwaller *JCAP* **07** (2019) 007, [[arXiv:1811.11175](#)].
- [51] G. D. Moore and T. Prokopec *Phys. Rev. Lett.* **75** (1995) 777–780, [[hep-ph/9503296](#)].
- [52] G. D. Moore and T. Prokopec *Phys. Rev.* **D52** (1995) 7182–7204, [[hep-ph/9506475](#)].
- [53] B. Laurent and J. M. Cline *Phys. Rev. D* **106** (2022), no. 2 023501, [[arXiv:2204.13120](#)].
- [54] B. Laurent and J. M. Cline *Phys. Rev. D* **102** (2020), no. 6 063516, [[arXiv:2007.10935](#)].
- [55] S. De Curtis, L. D. Rose, A. Guiggiani, A. G. Muyor, and G. Panico [arXiv:2201.08220](#).
- [56] S. De Curtis, L. Delle Rose, A. Guiggiani, A. Gil Muyor, and G. Panico *JHEP* **05** (2023) 194, [[arXiv:2303.05846](#)].
- [57] M. Barroso Mancha, T. Prokopec, and B. Swiezewska [arXiv:2005.10875](#).
- [58] S. Balaji, M. Spannowsky, and C. Tamarit *JCAP* **03** (2021) 051, [[arXiv:2010.08013](#)].
- [59] W.-Y. Ai, B. Garbrecht, and C. Tamarit [arXiv:2109.13710](#).
- [60] W.-Y. Ai, B. Laurent, and J. van de Vis [arXiv:2303.10171](#).

- [61] M. Dine, R. G. Leigh, P. Y. Huet, A. D. Linde, and D. A. Linde *Phys. Rev.* **D46** (1992) 550–571, [[hep-ph/9203203](#)].
- [62] D. Bodeker and G. D. Moore *JCAP* **0905** (2009) 009, [[arXiv:0903.4099](#)].
- [63] D. Bodeker and G. D. Moore *JCAP* **1705** (2017), no. 05 025, [[arXiv:1703.08215](#)].
- [64] S. Höche, J. Kozaczuk, A. J. Long, J. Turner, and Y. Wang *JCAP* **03** (2021) 009, [[arXiv:2007.10343](#)].
- [65] A. Azatov and M. Vanvlasselaer *JHEP* **09** (2020) 085, [[arXiv:2003.10265](#)].
- [66] Y. Gouttenoire, R. Jinno, and F. Sala *JHEP* **05** (2022) 004, [[arXiv:2112.07686](#)].
- [67] M. Barroso Mancha, T. Prokopec, and B. Swiezevska *JHEP* **01** (2021) 070, [[arXiv:2005.10875](#)].
- [68] I. Garcia Garcia, G. Koszegi, and R. Petrossian-Byrne [arXiv:2212.10572](#).
- [69] A. Azatov and M. Vanvlasselaer *JCAP* **01** (2021) 058, [[arXiv:2010.02590](#)].
- [70] G. R. Farrar and J. W. McIntosh, Jr. *Phys. Rev. D* **51** (1995) 5889–5904, [[hep-ph/9412270](#)].
- [71] A. Shkerin and S. Sibiryakov *JHEP* **11** (2021) 197, [[arXiv:2105.09331](#)].
- [72] M. E. Peskin and D. V. Schroeder, *An Introduction to quantum field theory*. Addison-Wesley, Reading, USA, 1995.
- [73] D. Tong *Part III Cambridge University Mathematics Tripos, Michaelmas* (2006).
- [74] M. L. Bellac, *Thermal Field Theory*. Cambridge Monographs on Mathematical Physics. Cambridge University Press, 3, 2011.